

Index

General analytic and computational procedures	2
Gene cloning	2
Heterologous expression, purification of enzymes and incubation experiments.....	5
Generation of enzyme variants by PCR-based site directed mutagenesis	7
Supplementary tables.....	8
Supplementary figures	13
NMR-spectra	24
References	47

General analytic and computational procedures

Chemicals were purchased from Sigma Aldrich Chemie GmbH (Steinheim, Germany), TCI (Zwijndrecht, Belgium) or Thermo Fisher (Karlsruhe, Germany) and used without purification. Solvents for column chromatography were purchased in p.a. grade and further purified by distillation. Thin-layer chromatography was performed with 0.2 mm precoated plastic sheets Polygram® Sil G/UV254 (Machery-Nagel (Düren, Germany)). Column chromatography was carried out using Merck (Darmstadt, Germany) silica gel 60 (70-200 mesh). ¹H NMR and ¹³C NMR spectra were recorded on a Bruker Avance III HD 700 MHz Cryo spectrometer, and were referenced against C₆D₆ ($\delta = 7.16$ ppm) for ¹H-NMR and C₆D₆ ($\delta = 128.06$ ppm) for ¹³C-NMR. GC-MS analyses were carried out with an Agilent (Santa Clara, USA) HP 7890B gas chromatograph fitted with a HP5-MS silica capillary column (30 m, 0.25 mm i. d., 0.50 μ m film) connected to a HP 5977A inert mass detector. Used MS parameters were 1) transfer line: 250 °C, and 2) electron energy: 70 eV. The GC parameters were 1) inlet pressure: 77.1 kPa, He 23.3 mL min⁻¹, 2) temperature program: 5 min at 50 °C increasing at 10 °C min⁻¹ to 320 °C, 3) injection volume: 1 μ L, 4) split ratio 10:1, 60 s valve time and 5) carrier gas: He at 1 mL min⁻¹. Retention indices (*I*) were determined from a homologous series of *n*-alkanes (C₈-C₄₀). Optical rotary powers were recorded on a P8000 Polarimeter (Krüss). Homology modeling was carried out by using the Swiss Model Server in fully automated mode. Amino acid sequence alignments were carried out using ClustalW as implemented in Geneious Pro 5.5.9.

Gene cloning

Putative terpene synthase genes were identified bioinformatically in the genome of *Termitomyces* sp. J132 (WGS Accession number: [JDCH000000000.1](#)) by using antiSMASH 3.0.¹ To obtain the coding sequences of terpene synthases STC4 and STC15, the following procedure was performed:

Termitomyces sp. T153 was grown on potatoe-dextrose agar (Carl Roth) plates for 20 days. Mycelium was harvested by aseptically scraping the agar plates with a sterile scalpel. The resulting mycelium was homogenized with mortar and pestle while cooling with liquid nitrogen. RNA extraction was performed according to the manufacturer's protocol of Isolate II RNA Plant Kit (BIOLINE). Samples were immediately stored at -80 °C. Starting from 1.0 μ g total RNA, cDNA was generated using the QuantiNova Reverse Transcription Kit (QIAGEN). Amplification of the target genes was done by PCR with S7 Phusion Polymerase (Biozym) on cDNA template: 95 °C 30 s, 30 cycles of 95 °C 30 s, 59.5 °C \pm 3.5 °C for 45 s and 72 °C for 1 min followed by a final extension at 72 °C for 5 min. For STC4 the primers STC4FW and STC4REV with annealing temperature 56°C were used, for STC15 the primers STC15FW and STC15REV with annealing temperature 59°C were used. For primer sequences cf. Table S1.

The blunt PCR products were purified by gel extraction (ZymoClean Gel DNA Recovery Kit), cloned in the pJET 1.2 blunt vector according to manufacturer's protocol (CloneJET PCR Cloning, ThermoScientific) and transformed into DH5 α cells. To verify the DNA sequences, PCR was performed with Phusion polymerase and pDNA as template (95 °C 30 s, 30 cycles of 95 °C 30 s, 70 °C for 45 s and 72 °C for 1 min followed by a final extension at 72 °C for 5 min, primers were provided with CloneJET PCR Cloning Kit). PCR-products were gel purified and send for sequencing at GATC.

Based on yet unpublished transcriptomic data and the annotated genome of *Termitomyces* sp. J123 (renamed as *Termitomyces* sp. P5, GenBank assembly accession: GCA_001263195.1), the cDNA gene sequence of STC9 was retrieved from NCBI and synthesized by BioCat (Heidelberg). The direct cloning from gDNA was not possible due to apparent intron sequences.

The target genes were amplified from the respective constructs and elongated with homology sequences to the expression plasmid pYE-Express² via PCR using Primers STC4-IB029f–STC4-IB030r for STC4, STC9-IB019f–STC9-IB020r for STC9 and STC15-IB027f–STC15-IB028r for STC15 (Table S1) for heterologous expression of the respective genes as N-terminally His-tagged proteins in *E. coli* BL21. pYE-Express was digested using HindIII and EcoRI. The linearized product and the respective PCR products were subjected to transformation in *Saccharomyces cerevisiae* FY834 by homologous recombination using the LiOAc/SS protocol.³ This cloning method provides higher efficiency than standard ligation. Plasmid DNA was isolated from grown yeast cultures using the Zymoprep Yeast Plasmid Miniprep II Kit (Zymo Research, Irvine, USA) following the instructions of the manufacturer.

The obtained plasmid constructs were transformed into *E. coli* BL 21 (DE3) via electroporation. Grown single colonies were checked by colony PCR and plasmids from positive clones were verified by sequencing of isolated plasmid DNA.

Sequence of the PCR Product STC4. Start and stop codon are marked in red.

```
ATGTTCAATTCCGCATCCCAGACCTCTTGAGCTGCCTGCCTGCATGCATAAAAGCTACAAA  
CGCGGACAACGACATTCTACAAGCAGGACTTGTGGAAGTGATCGACCAGTGTCACCTTGACTG  
ATCATTACAAAAGGACTTGAAACGTGCAGAAATACCTCATCTCGCTATCAGAGCATTCCCA  
GAATCGGATCTGAAATATTTGCGCATTTGCGTCAATATTTAATAGCTGCTTTTCTGCTAGA  
CCGGCTAACTGATAAACCCGCAACTGCCGCTCAGGCGCAGGAGTGGGCGGATATTTACAAGC  
AAGAGTTCAGAAAGACACTCCAAGGAACCAAGGGCTGCAAGGATCAATCAATATCTCACC  
AAGAAATGTGATATATAACCCGCAAGCGTTCAGCAAGACGTTTCGAAAAAACTAAAGGACCTGC  
AGAGATCATTAAATATTTGACCAGCCACATGTCGAACACCATCAAGGACCCTTACTGGTCTT  
GTCTGGTTCGAAAACAATATCCTCCTAGCAGACGGCATGGCAAAGAAGCTGTTCGATCGCGAA  
AATCCTGGTACTGAAATGGATCTGGAAACATATATAAAGGTTTCGAAGAGACACGATCGGCGC  
TCGCCAGCTATTCGATCTCGGGCGCTGGATCCATGAACTAAACATTACGCCGGAGACTCTGA  
CTCACCTGATATTGTTAGAATGGAAGAACAGTTCATTGACCTTATTTCTCTTGCAAATGAT
```

CTCTATTTCGTACAAGAAAGAATACCTCGCGAAAGACGCGAAGCATAATTACCTCACTATTGC
CCTTAGAGATCCTACTGTAGACCTGCACGAGAACGATTTACAGGGCGCGATCAACTACACTT
ACGATAAGTTCTGTGCGAGTCTTGGCAGATTTGGAACATCAAAAAGAAAGTGTACC GCGGTTC
AGGAAGAGCGAAGAGGCCAAAGTTGACAAGTACTTTTGGTTGATGATGAATGTTGTCATTGG
GACGATTCAGTGGAGTCTTGAGTGTGAGCGGTATGGTCATTTTGTGGATGCAGATGGACCGA
ATCAGGGAGATGTAGTCTTTAATCTTTAA

Sequence of the synthetic STC9 gene. The sequence is identical to the natural sequence. Start and stop codon are marked in red.

ATGTTTCAGGTTTCGATCATCCCAGCTCCTTCATCCTTCAGAATATCTGCGACATCACTGGCGC
TGTCTTTGAACTCAAAGAGAATCCTCTCCGCGAACAAGCTAATACTGCCGTTTTGAAATGGT
TTAAGGGATTCAACGTTTATGATAAAGCACAAAGGGGAGAAATTTATCAATGCTGGAAGATTC
GATATTTTTGCCGCTCTGAGCTTTCCGGAAGCAGATATTGAGCATCTCACGACTTGCCTCGC
ATTTTTCTCTGGGCATTTTCGACGGACGATCTCTCTGACGAGGGCGAATATCAGTCCAAAC
CAGAGAAGGTTTCGACGTGGACATGAAATATCCTGCAGCATCCTTCATGATGACTCCGCTCCT
CAACCAAGCTATCCGTATGCGGGTATGCTTTGGGACCTTCTTCGTCGCTTGCAGCCAATGG
GAAGTCAGGAATGTACAAGAGATTCAAGCAGGCATTCTTGGACTGGAGCTCATCACAAAGTCC
AGCAATCACTCAATAGGAATTTAGATCGAATTCCACCAGTCGATGAATTCATTCTTATGCGC
CGTTGTACAATTGGTGTCTGCGCTGGTTCGAAGCCATGGTTCGAATATTCCTCGATCTTGACAT
TCCTTCCTTTGTTTGGGAACATCCTGTAATCATCGGCATGTCACAAGTAACTTCAGATATTA
TGACTTGGCCCAATGATTTGTGCTCGTTCAATAAAGAACAGGCCGATGGGGACAACCAGAAC
TTTGTGTTGTGATTACAGCATGCTCACAATCTCAATCTTCAGGAGGCAGTTGATCTCTTGAC
CAAATGATAGCAGACCGAGTCCAAGATTACGTCAAGCTGAAAAAACGCCTACCATCTTTTG
GTCCTGACATAGACCCTGCCGTTATAAGTATGTGGATGCACCTGAGCAGTTTGTTC AAGGC
TGTGTTGTATGGTATTACTCCAGTCCCTCGCTATTTCCAGACATTGACCCAGGGGCAAATC
AAAAGCTGAAATACATCTCCTCTCAAAGCCAATCTCATCTGATCCAGTCCAAATGCACTACG
GGAGTGAACAACCAATCACCCTTGA

Sequence of the PCR Product STC15. Start and stop codon are marked in red.

ATGTCAGCCGCTACGAGCCAAC TATTACCTTCTGCCCTCGCGACTAAGATTATTTTACCCGA
TCTTGTGTCACATTTGTGACTTTCACACTTCGTTATAACCGTCATCGCAAGCAAATAACTCGCG
AGACGAAGCGGTGGCTGTTCAAGGGCGGTAATCTGAACGGGAAGAAGCGTGACGCCTTTCAT
GGTCTCAAGGCTGGGCTCCTCACGGCTATGACTTACCCGGACGCTGCATATCCCCAGCTCAG
AGTGTGTAATGACTTCCCTCACATACCTCTTCCACCTCGACAACCTCTCCGATGATATGGATA
ACCGCGGGACGCGTTTCGACCCGGATGTCGTGTTAAACTCTCTTCACCACCCTCATAACGTAT
TACGGTCCAGAACGAGTTGGGAAGATGACACGAGACTACTACAAACGGATGATCGTCACTGC
GTCACCTGGCGCTCAACAACGCTTCATTGAGACATTCGACTTTTTCTTTCAAAGCGTCACCC
AACAGGCTATAGATCGTGCGAATGGTGTCAATTCCTGATCTCGAGTCGTACATTGCCCTTCGC
CGCGATACTTCGGGGTGCAAGCCATGTTGGGCTCTCATTGAATACGCGAACAACCTCAACAT
TCCTGACGAGGTCATGGAGCATCCAATTATCGTGTCACTTGGGGAAGCCGCAAACGACCTTG
TTACATGGTCTAACGACATCTTCTCGTACAACGTGGAACAGTCGAAGGGTGACACGCACAAC
ATGATTCCAGTTGTAATGAATGAAGAGGGCCTCGATCTACAATCAGCTATTGACTTTGTCGG
GAACATGTGCAGACAGTCCATCGACCGCTTTGTTCGAAGATAGGGCTAACCTACCTTCATGGG
GTCCGGAAATCGACAAGGACGTAGCTGTTTACGTGAACGGGCTTGCGGACTGGATAGTGGGG

TCATTACATTGGTCATTCGAATCGGAAAGGTACTTTGGGAAGACTGGGCGGGAGGTTAAAGC
GAATCGCGTAGTCAACCTCCTTCCTCGACGTGCTTAA

Heterologous expression, purification of enzymes and incubation experiments

Analytical scale enzyme purifications and incubation experiments:

LB medium (100 mL, 50 µg/L kanamycin) was inoculated with 1% of an overnight culture of *E. coli* BL21 (DE3) carrying the respective expression plasmid and grown in LB medium (50 µg/L kanamycin). The culture was grown at 37 °C and 160 rpm until the OD₆₀₀ value reached 0.4 and cooled to 18 °C for 30 min. The culture was induced by addition of 400 µM IPTG and shaken at 18 °C at 160 rpm for 18 h. The cells were harvested by centrifugation (5100 g, 4 °C, 35 min) and resuspended in cell-lysis buffer (5 mL, 20 mM Na₂HPO₄, 0.5 M NaCl, 20 mM imidazole, 1 mM MgCl₂, pH 7.4). The cell suspension was ultra-sonicated for 3 min at 4 °C and the water soluble fraction was obtained by subsequent centrifugation (12.900 g, 10 min). The obtained clear solution was filtered through a 20 µm cellulose filter and subjected to Ni²⁺-NTA-affinity chromatography using Ni²⁺-NTA superflow (1 mL, Qiagen, Venlo, Netherlands). After binding and washing of the recombinant protein with binding buffer (2x 2 mL, 20 mM Na₂HPO₄, 0.5 M NaCl, 20 mM imidazole, 1 mM MgCl₂, pH 7.4), the His-tagged enzyme was eluted using elution buffer (2 mL, 20 mM Na₂HPO₄, 0.5 M NaCl, 0.5 M imidazole, 1 mM MgCl₂, pH 7.4). All wash and elution fractions were checked by SDS PAGE (see Figures S16-S18). Typical protein yields for all three enzymes were 1.5 – 2.0 mg per 100 mL expression culture. In case of experiments in D₂O the second washing and the elution was performed using the same buffers but on D₂O basis.

For subsequent test incubation the elution fraction (2 mL, containing ca. 1.5 mg of recombinant protein) was mixed with incubation buffer (2 mL, 20 mM Tris, 10 mM MgCl₂, 20% glycerol, pH 8.2) and incubated with farnesyl pyrophosphate trisammonium salt (1 mg, 0.5 mM), or the respective synthetic isotopomer.⁴ The incubation was carried out overnight and extracted either with C₆D₆ (0.5 mL) or hexane (0.5 mL), the extracts were dried with MgSO₄ and directly subjected to NMR or GC/MS analysis.

For comparative incubations of STC9 and its variants each elution fraction for a respective enzyme variant was brought to a concentration of 0.15 mg/mL using elution buffer (protein concentrations determined with Bradford assay). 600 µL of enzyme solution were mixed with 400 µL incubation buffer containing farnesyl pyrophosphate (0.25 mg, final concentration 0.5 mM) and incubated at 28°C for 2 h.

The aqueous solution was extracted with *n*-hexane (200 μ L), dried with MgSO_4 , and analyzed by GC-MS. The peak areas in the extracted ion chromatograms (EIC) for $m/z = 161$ at the retention time for **2** were integrated. All comparative incubations were carried out in triplicate. The average peak area obtained with the wild type enzyme was set to 100%.

Preparative scale enzyme purifications, incubation experiments and product isolations:

LB-medium (8x 1 L, 50 μ g/L kanamycin) was inoculated with 1% of an overnight culture of *E. coli* BL21 (DE3) carrying the respective expression plasmid and grown in LB medium (50 μ g/L kanamycin). The culture was grown at 37 $^{\circ}\text{C}$ and 160 rpm until the OD_{600} value reached 0.4 and cooled to 18 $^{\circ}\text{C}$ for 45 min. The culture was induced by addition of 400 μM IPTG and shaken at 18 $^{\circ}\text{C}$ at 160 rpm for 18 h. The cells were harvested by centrifugation (5100 g, 4 $^{\circ}\text{C}$, 35 min) and resuspended in cell lysis buffer (15 mL per 1 L harvested culture, 20 mM Na_2HPO_4 , 0.5 M NaCl, 20 mM imidazole, 1 mM MgCl_2 , pH 7.4). The cell suspension was ultra-sonicated in 30 mL portions for 6 min at 4 $^{\circ}\text{C}$ and the water soluble fraction was obtained by subsequent centrifugation (12.900 g, 4 $^{\circ}\text{C}$, 10 min). The obtained clear solution was filtered through a 20 μm cellulose filter and subjected to Ni^{2+} -NTA-affinity chromatography using Ni^{2+} -NTA superflow (20 mL, Qiagen, Venlo, Netherlands) in two portions of 60 mL. For each portion, after application and flowthrough of the solution, the material was flushed with binding buffer (2x 20 mL, 20 mM Na_2HPO_4 , 0.5 M NaCl, 20 mM imidazole, 1 mM MgCl_2 , pH 7.4) before the enzyme was eluted using elution buffer (2x 20 mL, 20 mM Na_2HPO_4 , 0.5 M NaCl, 0.5 M imidazole, 1 mM MgCl_2 , pH 7.4). The protein content of the elution fractions was determined by Bradford assays, typically yielding ca. 3 mg mL^{-1} protein for all three enzymes.

The collected elution fractions (80 mL) were mixed with incubation buffer (80 mL, 20 mM Tris, 10 mM MgCl_2 , 20% glycerol, pH 8.2) and farnesyl pyrophosphate trisammonium salt (80 mg, 0.185 mmol) dissolved in incubation buffer (20 mL) was added dropwise over 1 h using a syringe pump. The incubation was carried out overnight, followed by extraction with pentane (3x 80 mL). The combined organic layers were dried with MgSO_4 , filtrated and concentrated *in vacuo*. The crude product was purified by column chromatography.

Product of STC4 – (+)-intermedeol (**1**):

Column chromatography: pentane/ Et_2O (5:1), **yield:** 0.5 mg (1.2 %).

NMR: See Table S3. **Optical rotary power:** $[\alpha]_{\text{D}}^{20.0} = +13.3$ (c 0.03, CH_2Cl_2). **GC** (HP-5): $I = 1692$. **EI-MS** (70 eV): m/z (%) = 222 (1), 205 (14), 204 (88), 190 (13), 189 (88), 175 (18), 162 (17), 161 (100), 149 (11), 148 (14), 147 (39), 137 (18), 135 (27),

134 (12), 133 (37), 125 (33), 123 (37), 122 (49), 121 (33), 119 (23), 109 (37), 108 (17), 107 (47), 105 (41), 96 (12), 95 (38), 94 (11), 93 (42), 91 (29), 83 (12), 82 (22), 81 (57), 79 (28), 77 (13), 71 (31), 69 (18), 68 (10), 67 (28), 55 (22), 53 (9), 43 (30), 41 (17).

Product of STC9 – (–)- γ -cadinene (**2**):

Column chromatography: pentane, **yield:** 2.3 mg (6.1 %).

NMR: See Table S4. **Optical rotary power:** $[\alpha]_D^{20.0} = -9.0$ (*c* 0.2, CH₂Cl₂). **GC** (HP-5): *I* = 1537. **EI-MS** (70 eV): *m/z* (%) = 204 (24), 162 (10), 161 (100), 133 (18), 120 (10), 119 (25), 105 (32), 93 (19), 91 (19), 81 (13), 79 (12).

Product of STC15 – (+)-germacrene D-4-ol (**3**):

Column chromatography: pentane/ Et₂O (5:1), **yield:** 0.5 mg (1.2 %).

NMR: See Table S5. **Optical rotary power:** $[\alpha]_D^{20.0} = +83.0$ (*c* 0.03, C₆D₆). **GC** (HP-5): *I* = 1581. **EI-MS** (70 eV): *m/z* (%) = 222 (1), 207 (7), 204 (16), 161 (49), 133 (9), 123 (19), 121 (12), 119 (20), 109 (12), 107 (9), 105 (30), 95 (14), 93 (17), 91 (14), 82 (9), 81 (100), 80 (16), 79 (14), 71 (11), 69 (11), 67 (10), 55 (12), 43 (24), 41 (13).

Generation of enzyme variants by PCR-based site directed mutagenesis

The variants of the described enzymes were obtained by PCR using the mutagenesis primers listed in Table S2 additionally to the primers listed in Table S1.

In a representative procedure for STC4 W335A three PCRs were conducted. To obtain two fragments containing the mutation, a PCR of the template gene on pYE-express with the primer pair STC4-IB029f/STC4-W335Ar and a PCR with the primer pair STC4-IB029r/STC4-W335Af were carried out. The two resulting gene fragments were used together as a template in a third PCR in combination with the primer pair STC4-IB030f/STC4-IB030r, which combined the fragments and introduced the homology regions for pYE-Express. The resulting PCR product (STC4 W335A) was cloned into pYE-Express and heterologously expressed as described above. The procedure was repeated for each mutation using the respective primers from Tables S1 and S2.

For doubly mutated genes, a gene containing one of the desired mutations was used as a template and the same procedure as for singly mutated enzymes was run through with mutational primers for the second desired mutation.

Table S2: Primers used for introduction of point mutations.

Primer	Sequence
STC4-W335Af	CGATTCAGGCGAGTCTTG
STC4-W335Ar	CAAGACTCGCCTGAATCG
STC4-W335Ff	GACGATTCAGTTTAGTCTTGAGT
STC4-W335Fr	ACTCAAGACTAAACTGAATCGTC
STC9-W314Af	CTGTGTTGTAGCGTATTACTCCA
STC9-W314Ar	TGGAGTAATACGCTACAACACAG
STC9-W314Ff	GCTGTGTTGTATTTTATTACTCCAG
STC9-W314Fr	CTGGAGTAATAAAATACAACACAGC
STC15-W314Af	GTCATTACATGCGTCATTCGAATC
STC15-W314Ar	GATTCGAATGACGCATGTAATGAC
STC15-W314Ff	GGGTCATTACATTTTTCATTCGAATCG
STC15-W314Fr	CGATTCGAATGAAAAATGTAATGACCC
STC9-C311Hf	GTTCAAGGCCATGTTGTATGG
STC9-C311Hr	CCATACAACATGGCCTTGAAC
STC9-C311Nf	GTTCAAGGCAATGTTGTATGG
STC9-C311Nr	CCATACAACATTGCCTTGAAC
STC9-C311Sf	GTTCAAGGCTCTGTTGTATGG
STC9-C311Sr	CCATACAACAGAGCCTTGAAC
STC9-Y315Gf	GTTGTATGGGGTTACTCCAGTC
STC9-Y315Gr	GACTGGAGTAACCCATACAAC
STC9-Y315Sf	TGTTGTATGGTCTTACTCCAGTC
STC9-Y315Sr	GACTGGAGTAAGACCATACAACA

Table S3: NMR data of (+)-intermedeol (**1**) in C₆D₆ at 298 K. All shown data are in line with the literature.⁵

C ^a		¹ H ^b	¹³ C ^b
1	CH ₂	1.22-1.18 (m) 0.98 (ddd, ² J = 12.8, ³ J = 5.4, ³ J = 5.4)	41.7
2	CH ₂	1.34-1.31 (m)	20.5
3	CH ₂	1.58-1.54 (m) 1.18-1.13 (m)	43.8
4	C _q	–	71.3
5	CH	1.38-1.34 (m)	49.1
6	CH ₂	2.15 (ddt, ² J = 13.5, ³ J = 2.1, ³ J = 2.1) 1.27 (ddd, ² J = 13.5, ³ J = 5.2, ³ J = 5.2)	23.1
7	CH	2.33 (br s)	39.8
8	CH ₂	1.80 (m) 1.61 (ddt, ² J = 14.3, ³ J = 4.1, ³ J = 5.8)	23.9
9	CH ₂	1.41 (ddd, ² J = 13.2, ³ J = 3.8, ³ J = 3.8) 1.04 (ddd, ² J = 12.9, ³ J = 3.5, ³ J = 3.5)	40.7
10	C _q	–	35.4
11	C _q	–	111.4
12	CH ₃	1.77 (br s)	23.0
13	CH ₂	5.08 (br s) 5.06-5.04 (m)	146.9
14	CH ₃	0.96 (d, ⁴ J = 0.6)	22.7
15	CH ₃	0.79 (br s)	18.6

^aCarbon numberings as shown in Figure 1 in the main text; ^bchemical shifts are given in ppm, coupling constants are given in Hertz, multiplicity: m = multiplet, s = singlet, d = doublet, t = triplet, q = quartet, br = broad.

Table S4: NMR data of (–)- γ -cadinene (**2**) in C₆D₆ at 298 K. All shown data are in line with the literature.⁶

C ^a		¹ H ^b	¹³ C ^b
1	CH	1.79-1.75 (m)	44.6
2	CH ₂	1.94-1.90 (m) 1.55-1.48 (m)	26.2
3	CH ₂	1.98-1.94 (m) 1.89-1.82 (m)	30.8
4	C _q	–	134.6
5	CH	5.64 (br s)	122.9
6	CH	1.77-1.73 (m)	45.5
7	CH	1.22-1.17 (m)	47.3
8	CH ₂	1.68-1.64 (m) 1.12 (dq, ² J = 12.4, ³ J = 4.1)	26.9
9	CH ₂	2.38 (ddd, ² J = 12.9, ³ J = 4.0, ³ J = 2.9) 2.00 (ddd, ² J = 13.0, ³ J = 4.8, ³ J = 1.4)	36.7
10	C _q	–	153.1
11	CH	2.16 (ddq, ³ J = 7.0, ³ J = 7.0, ³ J = 3.5)	26.5
12	CH ₃	0.73 (d, ³ J = 7.0)	15.3
13	CH ₃	0.88 (d, ³ J = 7.0)	21.7
14	CH ₂	4.82 (br s, H _E) 4.71-4.69 (m, H _Z)	103.8
15	CH ₃	1.65 (br s)	24.1

^aCarbon numberings as shown in Figure 1 in the main text; ^bchemical shifts are given in ppm, coupling constants are given in Hertz, multiplicity: m = multiplet, s = singlet, d = doublet, t = triplet, q = quartet, br = broad.

Table S5: NMR data of (+)-germacrene-D-4-ol (**3**) in C₆D₆ at 298 K. All shown data are in line with the literature.^{4b}

C ^a		¹ H ^b	¹³ C ^b
1	CH	4.92 (br d, ³ J = 11.5),	129.4
2	CH ₂	2.65-2.57 (m) 1.90-1.87 (m)	24.2
3	CH ₂	1.44 (ddd, ³ J = 3.7, ³ J = 4.0, ² J = 13.7) 1.33-1.29 (m)	40.0
4	C _q	–	72.7
5	CH	5.01(d, ³ J = 15.8),	140.5
6	CH	5.25 (dd, ³ J = 15.7, ³ J = 10.0)	126.0
7	CH	1.94-1.89 (m)	53.1
8	CH ₂	1.34-1.28 (m) 1.28-1.22 (m)	26.5
9	CH ₂	2.27-2.24 (m) 2.24-2.21 (m)	41.7
10	C _q	–	132.4
11	CH	1.41-1.36 (m)	33.4
12	CH ₃	0.90 (d, ³ J = 6.8)	20.9
13	CH ₃	0.86 (d, ³ J = 6.9)	19.3
14	CH ₃	1.07 (s)	31.3
15	CH ₃	1.54 (t, ⁴ J = 1.3)	16.8

^aCarbon numberings as shown in Figure 1 in the main text; ^bchemical shifts are given in ppm, coupling constants are given in Hertz, multiplicity: m = multiplet, s = singlet, d = doublet, t = triplet, q = quartet, br = broad.

Supplementary figures

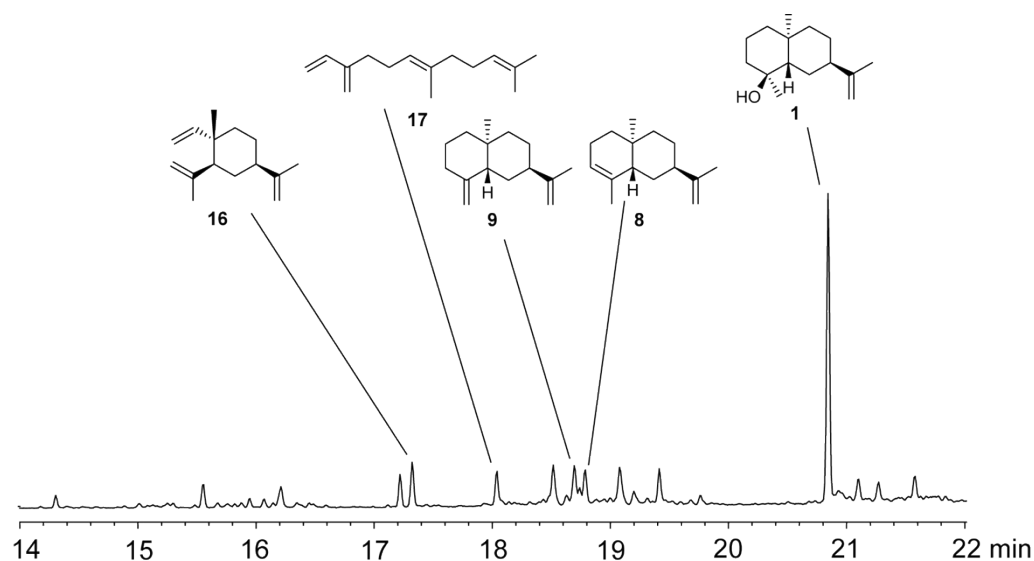


Figure S1: GC-MS analysis of the extract obtained from the incubation experiment with STC4 using FPP as the substrate. Compound **17** represents a spontaneously formed lysis product of FPP also observed in control experiments without enzyme.

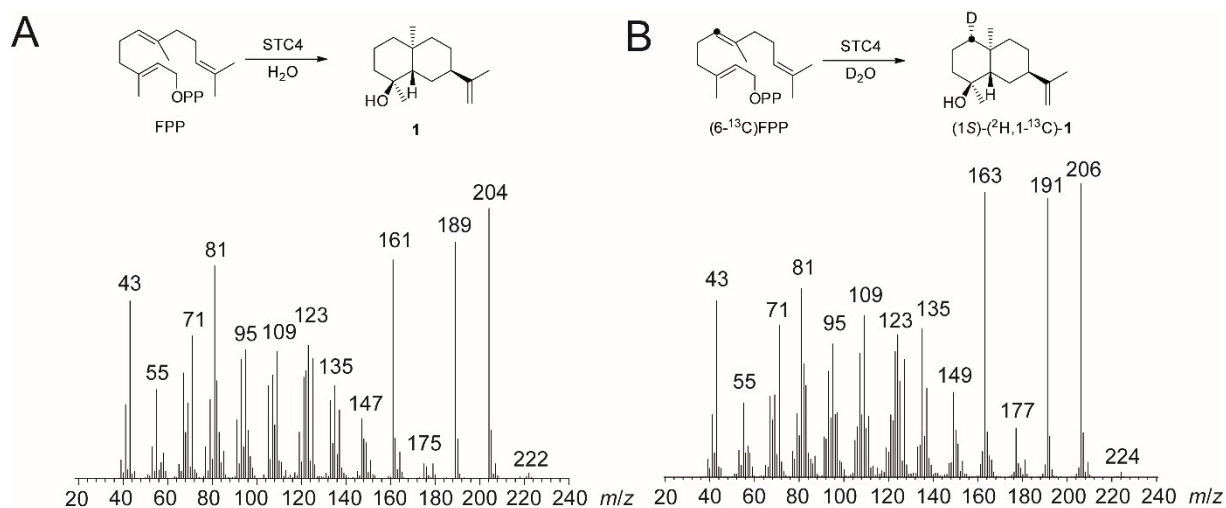


Figure S2: Mass spectral analysis of **1**. **A:** After incubation of non-labeled FPP in H₂O; **B:** After incubation of (6-¹³C)FPP in D₂O.

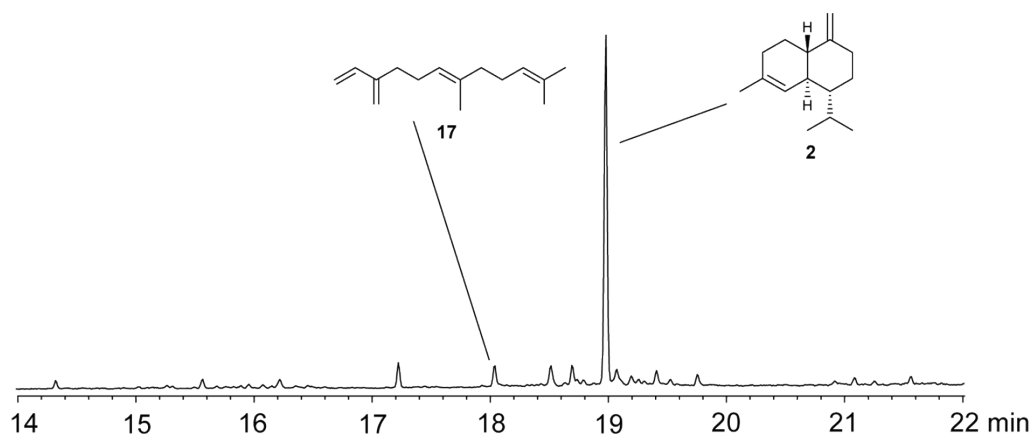


Figure S3: GC-MS analysis of the extract obtained from the incubation experiment with STC9 using FPP as the substrate. Compound **17** represents a spontaneously formed lysis product of FPP also observed in control experiments without enzyme.

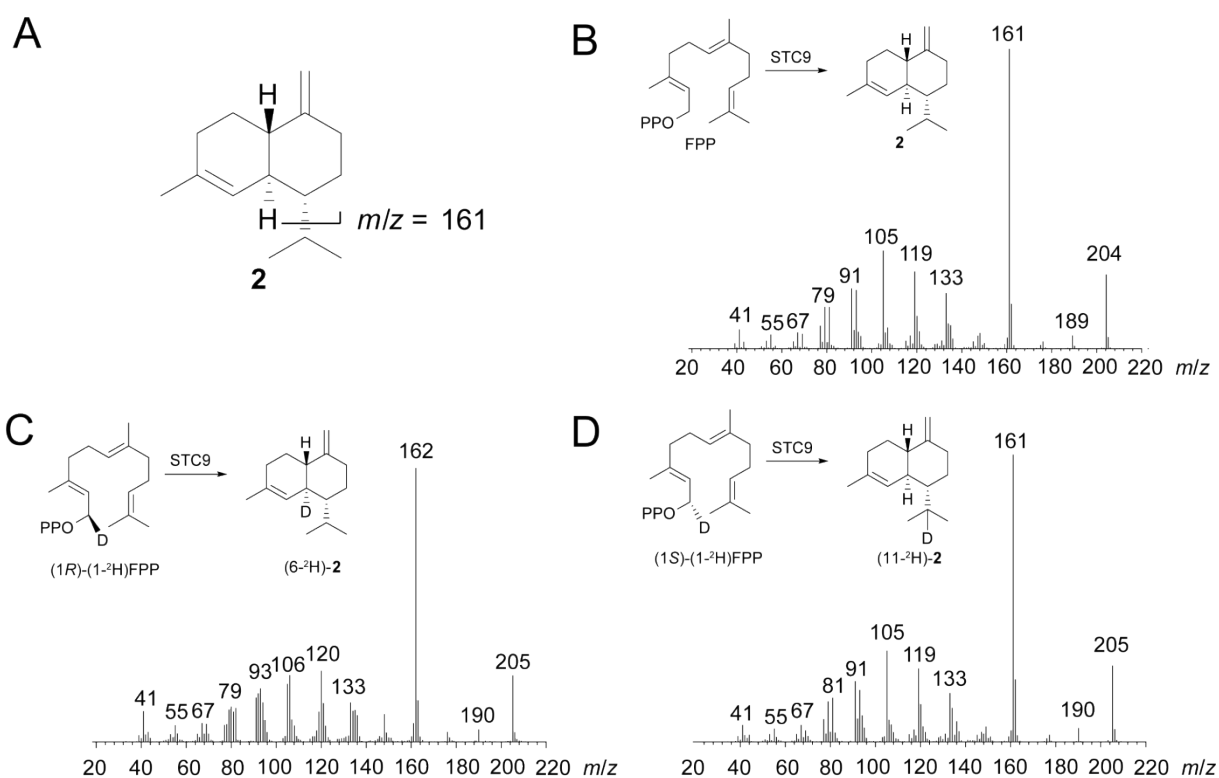
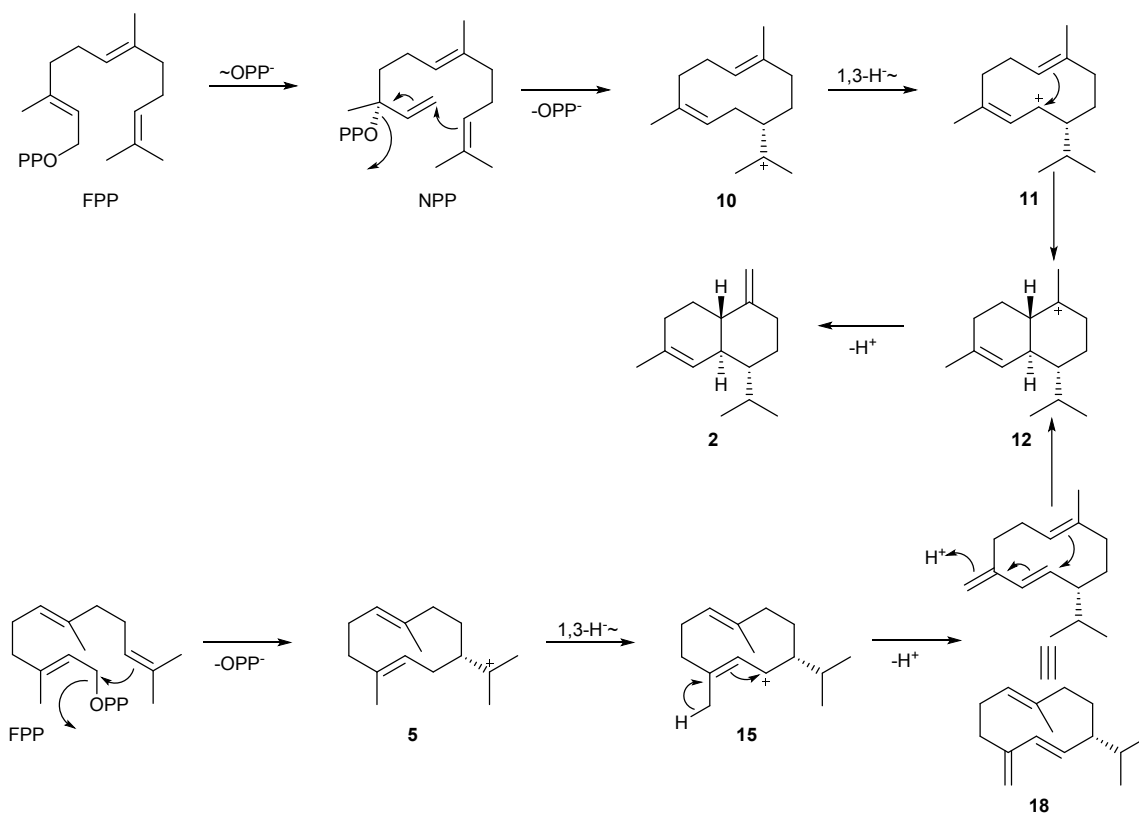


Figure S4: Mass spectrometry analysis of the stereoselective 1,3-hydride shift in the cyclization mechanism of STC9. **A:** Fragmentation to the ion responsible for the basepeak ($m/z = 161$); **B:** mass spectrum of **2** after incubation with unlabeled FPP; **C:** mass spectrum of labeled **2** after incubation with (1R)-(1-²H)FPP; **D:** mass spectrum of labeled **2** after incubation with (1S)-(1-²H)FPP.



Scheme S1: Cyclization of FPP towards **2**. The upper path shows the reaction sequence as shown in the main text, proceeding via isomerization to NPP and **10**. The lower path shows an alternative path via direct formation of **5**, 1,3-hydride shift to **15** followed by deprotonation to yield germacrene D (**18**). Germacrene D (**18**) could change its conformation and by re-protonation result in cation **12**, which after deprotonation yields **2**. Both alternative pathways have been suggested by Arigoni.⁷ Since re-protonation in an incubation experiment using D_2O should produce a different mass spectrum of the resulting product due to incorporation of deuterium, which was not observed, the lower path for formation of **2** by STC9 is disfavored. The outcome was the same for the cadinenes produced by STC15.

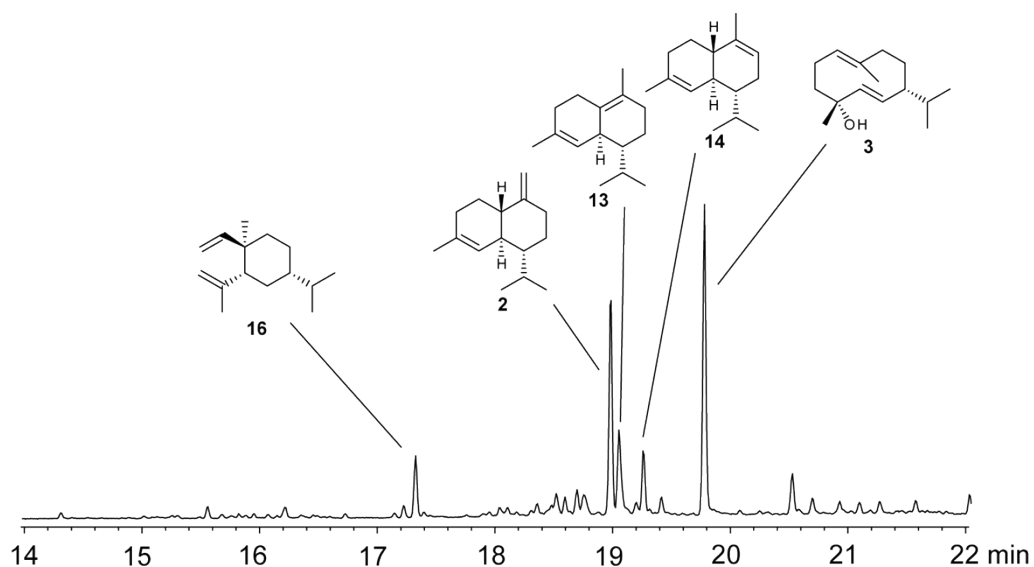


Figure S5: GC-MS analysis of the extract obtained from the incubation experiment with STC15 using FPP as the substrate.

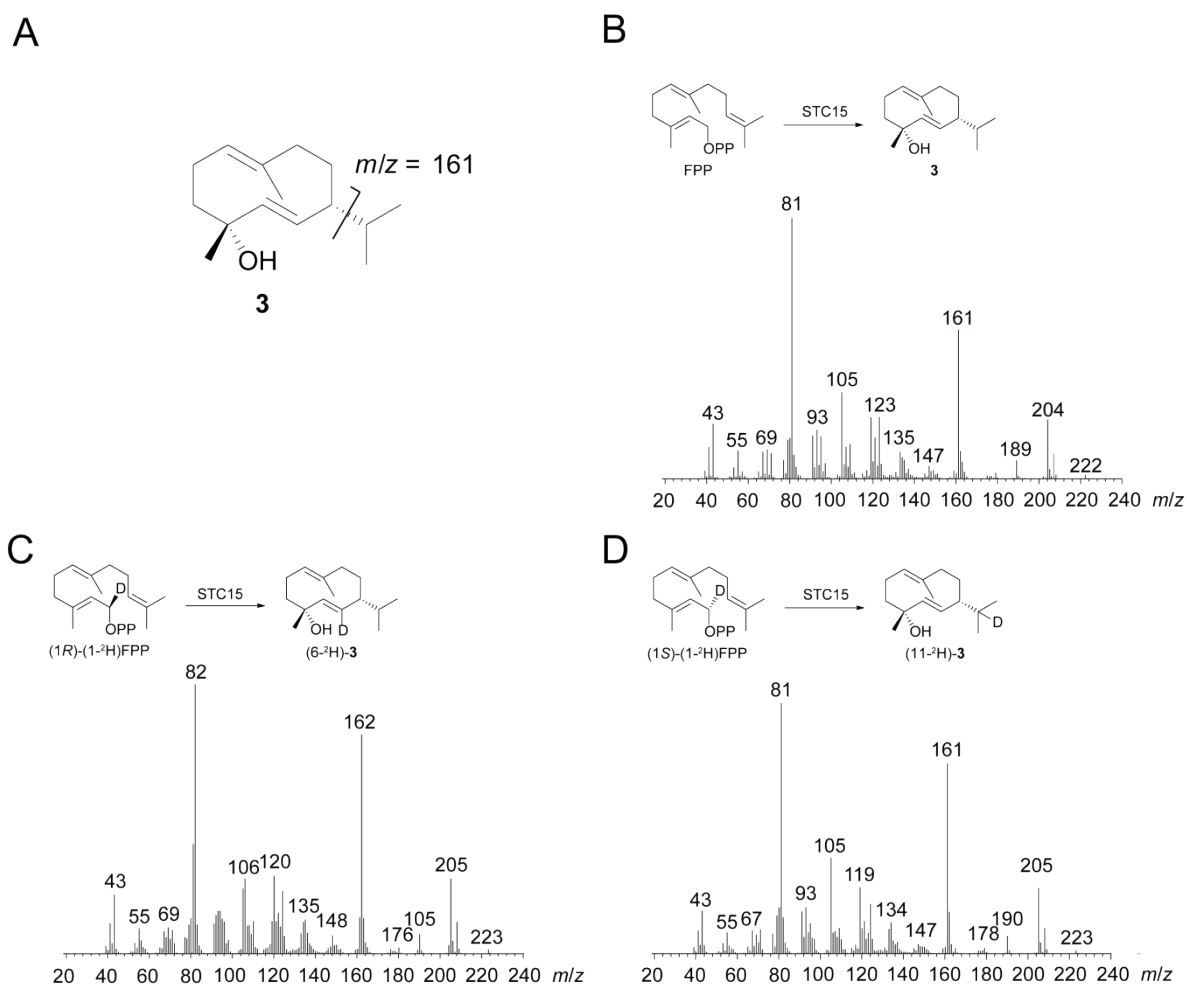


Figure S6: Mass spectrometry analysis of the stereoselective 1,3-hydride shift in the cyclization mechanism of STC15 towards **3**. **A:** Fragmentation to the ion responsible for the signal at $m/z = 161$; **B:** mass spectrum of **3** after incubation with unlabeled FPP; **C:** mass spectrum of labeled **3** after incubation with (1*R*)-(1-²H)FPP; **D:** mass spectrum of labeled **3** after incubation with (1*S*)-(1-²H)FPP.

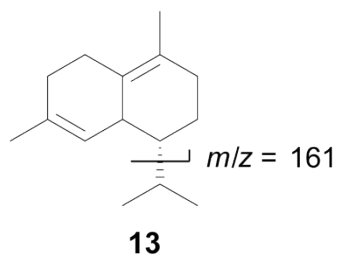
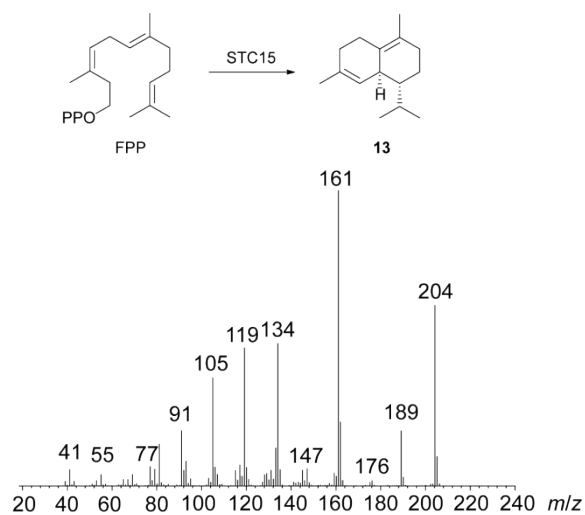
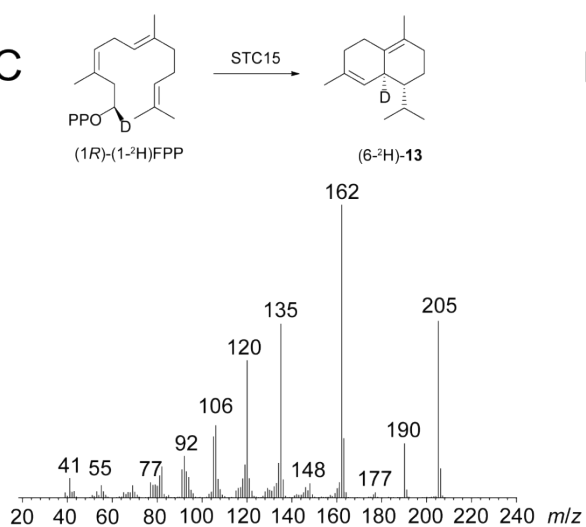
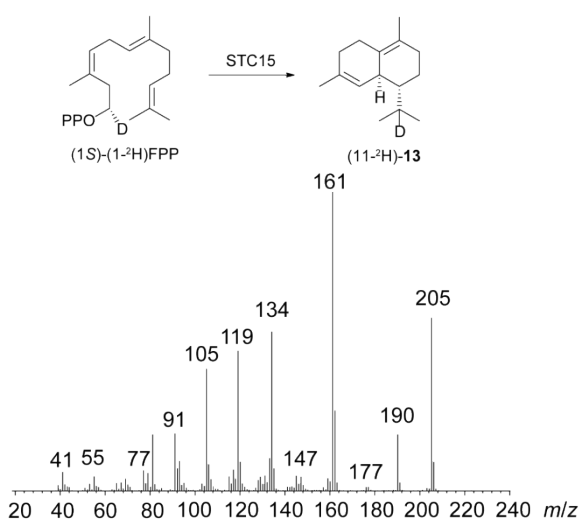
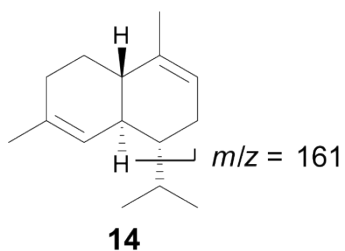
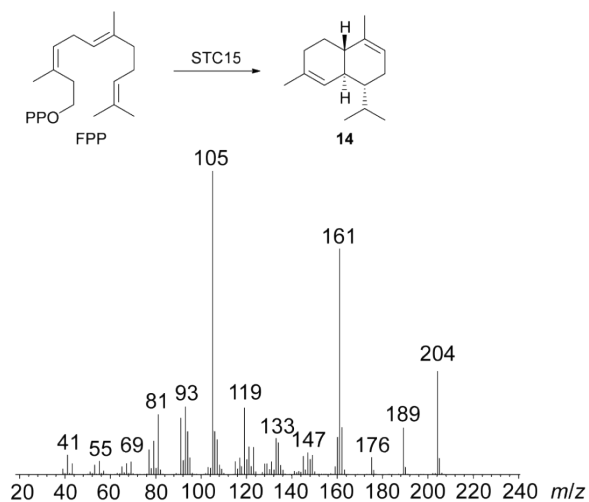
A**B****C****D**

Figure S7: Mass spectrometrical analysis of the stereoselective 1,3-hydride shift in the cyclization mechanism of STC15 towards **13**. **A:** Fragmentation to the ion responsible for the signal at $m/z = 161$; **B:** mass spectrum of **13** after incubation with unlabeled FPP; **C:** mass spectrum of labeled **13** after incubation with (1R)-(1-²H)FPP; **D:** mass spectrum of labeled **13** after incubation with (1S)-(1-²H)FPP.

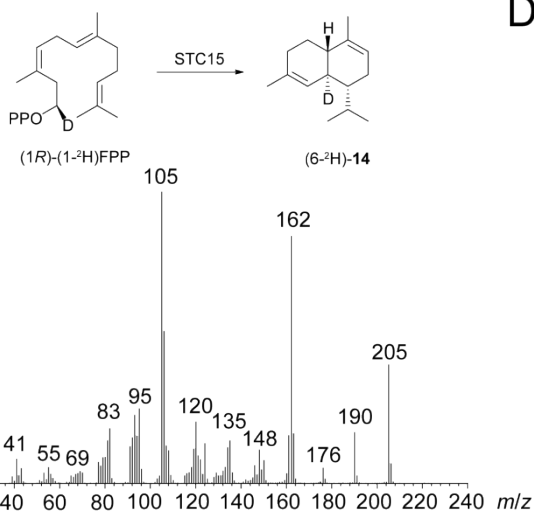
A



B



C



D

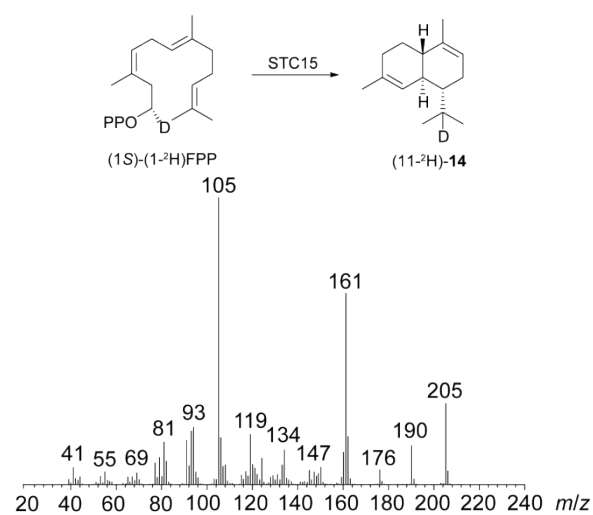
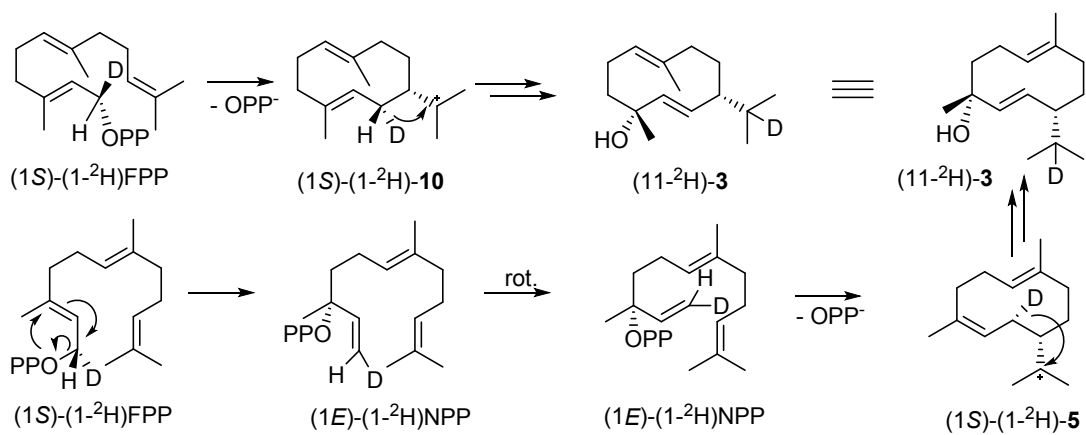


Figure S8: Mass spectrometrical analysis of the stereoselective 1,3-hydride shift in the cyclization mechanism of STC15 towards **14**. **A:** Fragmentation to the ion responsible for the signal at $m/z = 161$; **B:** mass spectrum of **14** after incubation with unlabeled FPP; **C:** mass spectrum of labeled **14** after incubation with (1*R*)-(1-²H)FPP; **D:** mass spectrum of labeled **14** after incubation with (1*S*)-(1-²H)FPP.



Scheme S2: Possible cyclization steps from FPP to **3** via direct 1,10-cyclization (up) or via isomerization to NPP first (down). In both cases the *pro-S* hydrogen migrates to C-11 in **3**, here illustrated by the reaction of (1S)-(1-2H)FPP.

10 20 31 40 50 60
 MVQFRIPDLLSCLPACIKATNADNDILQAGLVEVIDQCHLTDHYKKDLKRARIPHLAIRAFP
 70 80 90 100 110 120
 NSDLKYLRICVEYLIAAFL**LDRLTD**KPATAAQAQEWADIYKQEFRKTLQGTKGPARINQYLT
 130 140 150 160 170 180
 KKCDIYPQAFSKTFEKTGPAEIIKYLTSHMSNTIKDPYWSCLVENNILLADGMAKEAVDRE
 190 200 210 220 230 240
 NPGTEMDLETYIKV**RR**DTIGARQLFDLGRWIHELNITPETLTHPDIVRMEEQFIDLIS**LAND**
 250 260 270 280 290 300 3
LYSYKKEYLAKDAKHNYLTIALRDPTVDLHENDLQGAINYTYDKFCRVLADLEHQKKVLPRF
 10 320 330 340 350 360
 RKSEEAKVDKYFWLMMNVVIGTI**QWS**LECE**RY**GHFVDADGPNQGDVVFNL*

Figure S9: Amino acid sequence of STC4. Conserved aspartate rich motif (DDXXD, here altered to DXXXD), NSE triad, RY pair, pyrophosphate sensor and the conserved W335 mutated in this work are marked in bold.

10 20 31 40 50 60
 MFRFDHPSSFILQNICDITGAVFELKENPLREQANTAVLKWFKGFNVYDKAQGEKFINAGRF
 70 80 90 100 110 120
 DIFAALSFPEADIEHLTTCLAFFLWAFST**DDL**SDEGEYQSKPEKVRRGHEISCSILHDDSAP
 130 140 150 160 170 180
 QPSYPYAGMLWDLRLRRLRANGKSGMYKRFKQAFLDWSSSQVQQLNRNLDRIPPVDEFIL**MR**
 190 200 210 220 230 240
 RCTIGAALVEAMVEYSLDLDIPSFVWEHPVIGMSQVTSDIMTWP**NDLCSFNKE**QADGDNQN
 250 260 270 280 290 300 3
 FVCVLQHAHNLNLQEAVDLLTKMIADRVQDYVKLKKRLPSFGPDIDPAVHKYVDALEQFVQG
 10 320 330 340 350 360
CVVWYYSS**PRY**FPDIDPRGKSKAEIHLLSKPISSDPVQMHYGSETTNHP*

Figure S10: Amino acid sequence of STC9. Conserved aspartate rich motif, NSE triad, RY pair, pyrophosphate sensor and the conserved W314 as well as the putative active site residues C311 and Y315 that are mutated in this work are marked in bold.

10 20 31 40 50 60
 MSAATSQLLPSALATKIILPDLVAHCDFTLRYNRHRKQITRETKRWLFKGGNLNGKKRDAFH
 70 80 90 100 110 120
 GLKAGLLTAMTYPDAAYPQLRVCNDFLTLYLFHLDNLS**DDMD**NRGTRSTADVVLNSLHHPHTY
 130 140 150 160 170 180
 YGPERVGMTRDYYKRMIVTASPGAQQRFIETFDFFFQSVTQQAIDRANGVIPDLESYIAL**R**
 190 200 210 220 230 240
 RDTSGCKPCWALIEYANNLNIPDEVMEHPPIIVSLGEAANDLVTWS**NDIFS**YNVEQSKGDTHN
 250 260 270 280 290 300 3
 MIPVVMNEEGLDLQSAIDFVGNMCRQSIDRFVEDRANLPSWGPEIDKDVAVYVNGLADWIVG
 10 320 330 340
 SLH**W**SFESE**RY**FGKTGREVKANRVVNNLLPRRA*

Figure S11: Amino acid sequence of STC15. Conserved aspartate rich motif (DDXXD, here altered to DDXD), NSE triad, RY dimer and the conserved W314 mutated in this work are marked in bold.

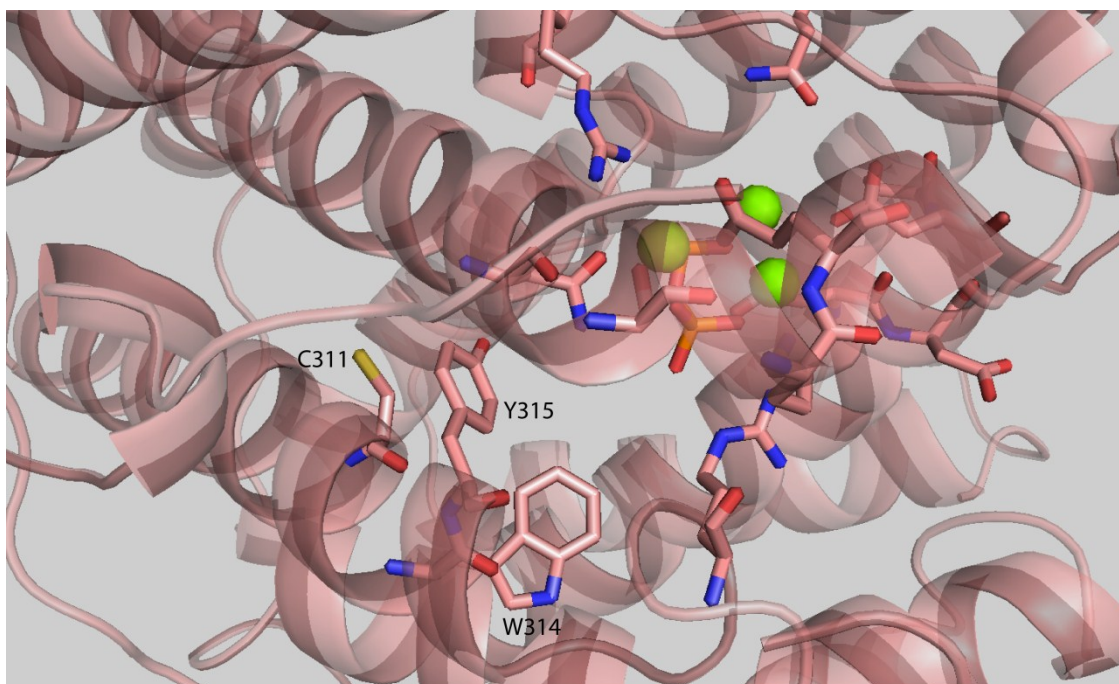


Figure S12: Active site in homology model of STC9 from *Termitomyces* based on the crystal structure of selinadiene synthase from *S. pristinaespiralis* (PDB code 4OKM).⁸ The upper right part shows residues responsible for coordination of the trinuclear Mg^{2+} cluster (green spheres, superimposed from the selinadiene synthase crystal structure) and the pyrophosphate moiety (orange sticks, superimposed from the selinadiene synthase crystal structure). Cystein 311 and tyrosin 315 in the direct neighbourhood of the highly conserved tryptophan 314 point towards the inside of the active site and were targeted by site directed mutagenesis. Image was created using Pymol.

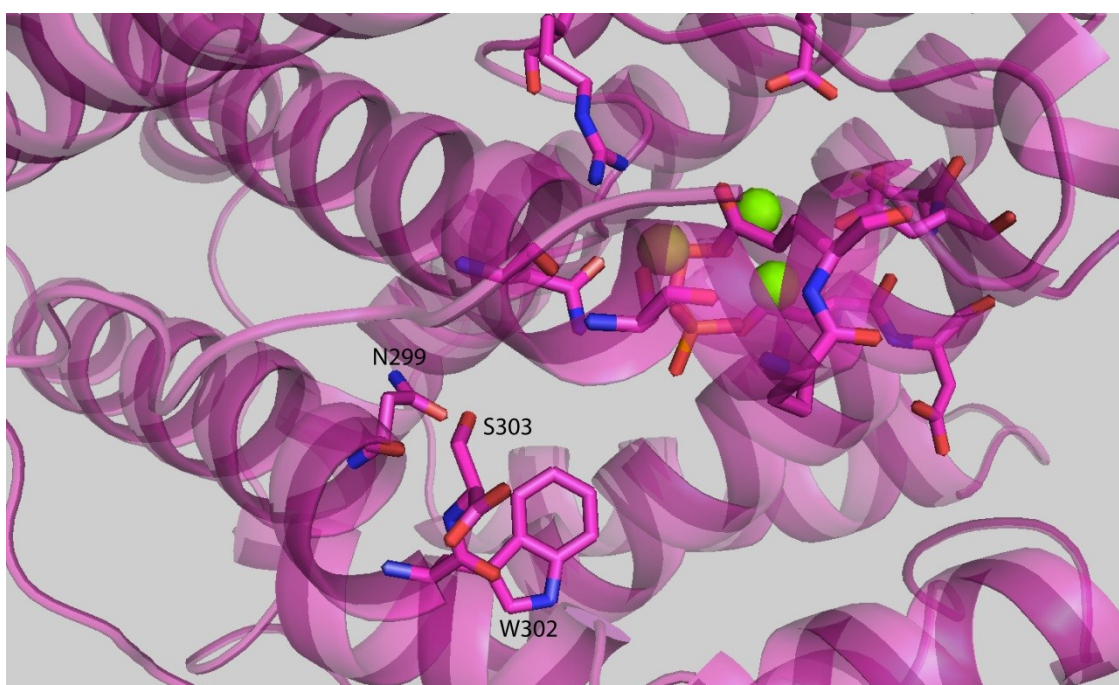


Figure S13: Active site in homology model of $(-)\text{-}\gamma\text{-cadinene}$ synthase from *C. pinensis*^{4b} based on the crystal structure of selinadiene synthase from *S. pristinaespiralis* (PDB code 4OKM).⁸ The upper right part shows residues responsible for coordination of the trinuclear Mg^{2+} cluster (green spheres, superimposed from the selinadiene synthase crystal structure) and the pyrophosphate moiety (orange sticks, superimposed from the selinadiene synthase crystal structure). Asparagin 299 and serine 303 in the direct neighbourhood of the highly conserved tryptophan 302 point towards the inside of the active site. Image was created using Pymol.

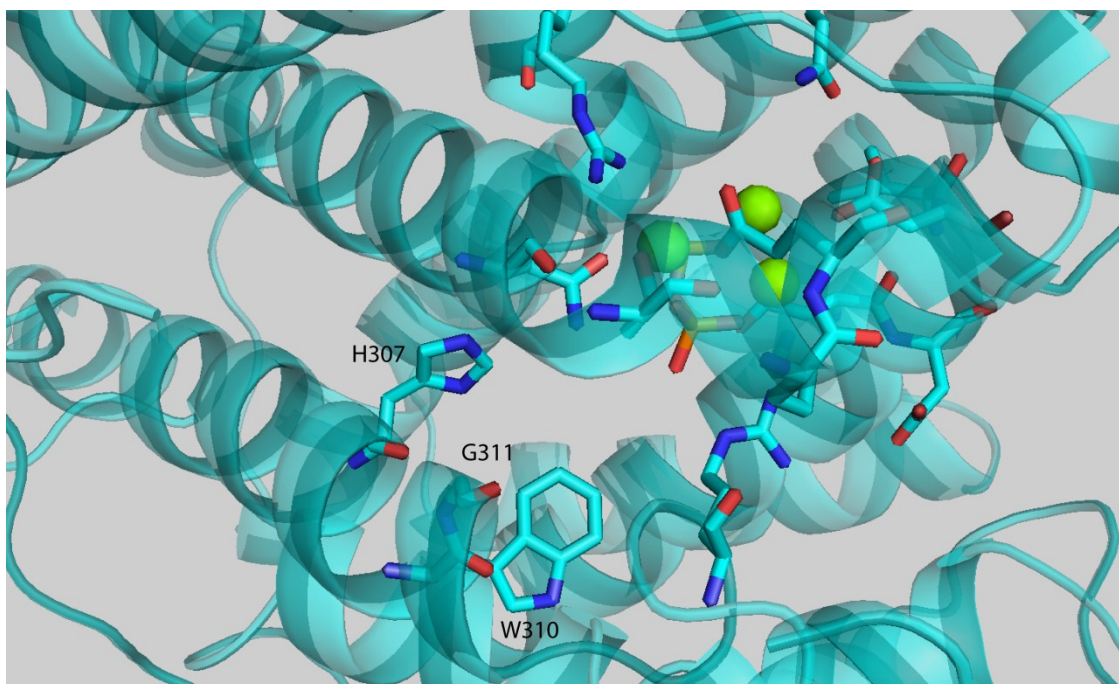


Figure S14: Active site in homology model of (-)- δ -cadinene synthase from *S. clavuligerus*⁹ based on the crystal structure of selinadiene synthase from *S. pristinaespiralis* (PDB code 4OKM).⁸ The upper right part shows residues responsible for coordination of the trinuclear Mg^{2+} cluster (green spheres, superimposed from the selinadiene synthase crystal structure) and the pyrophosphate moiety (orange sticks, superimposed from the selinadiene synthase crystal structure). Histidin 307 and glycine 311 in the direct neighbourhood of the highly conserved tryptophan 310 point towards the inside of the active site. Image was created using Pymol.

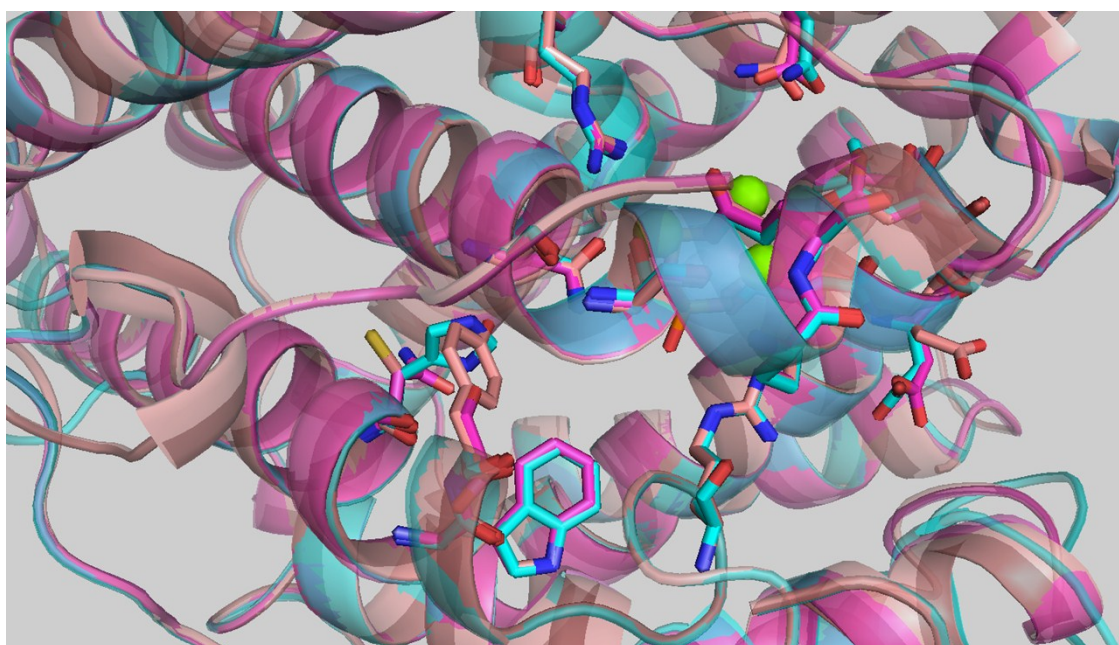


Figure S15: Superimposition of the three homology models from Figures S12 – S14. Image was created using Pymol.

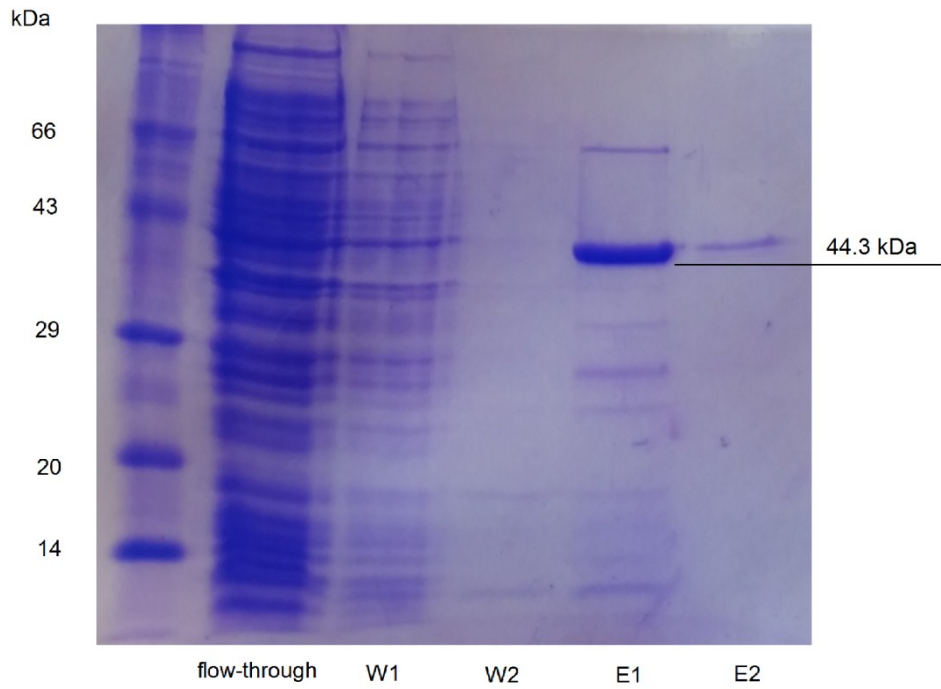


Figure S16: SDS-PAGE gel of STC4 purification. W1: first washing fraction; W2: second washing fraction; E1: first elution fraction; E2: second elution fraction.

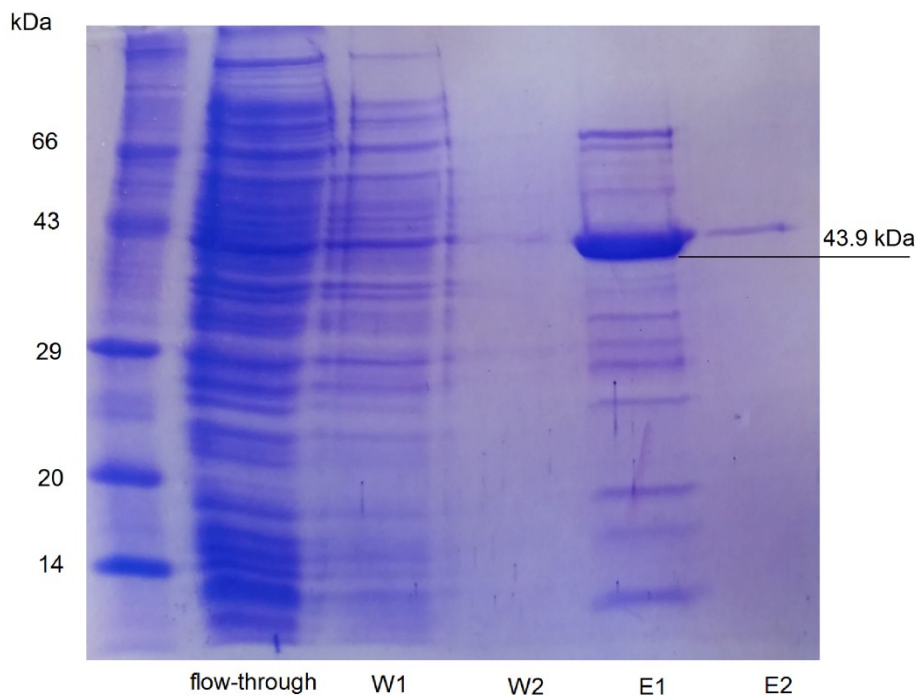


Figure S17: SDS-PAGE gel of STC9 purification. W1: first washing fraction; W2: second washing fraction; E1: first elution fraction; E2: second elution fraction.

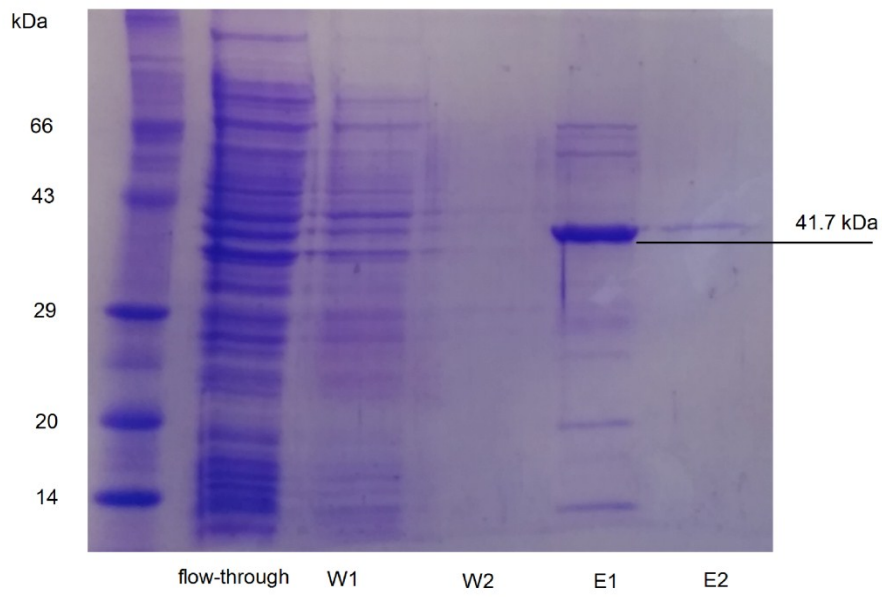


Figure S18: SDS-PAGE gel of STC15 purification. W1: first washing fraction; W2: second washing fraction; E1: first elution fraction; E2: second elution fraction.

NMR-spectra

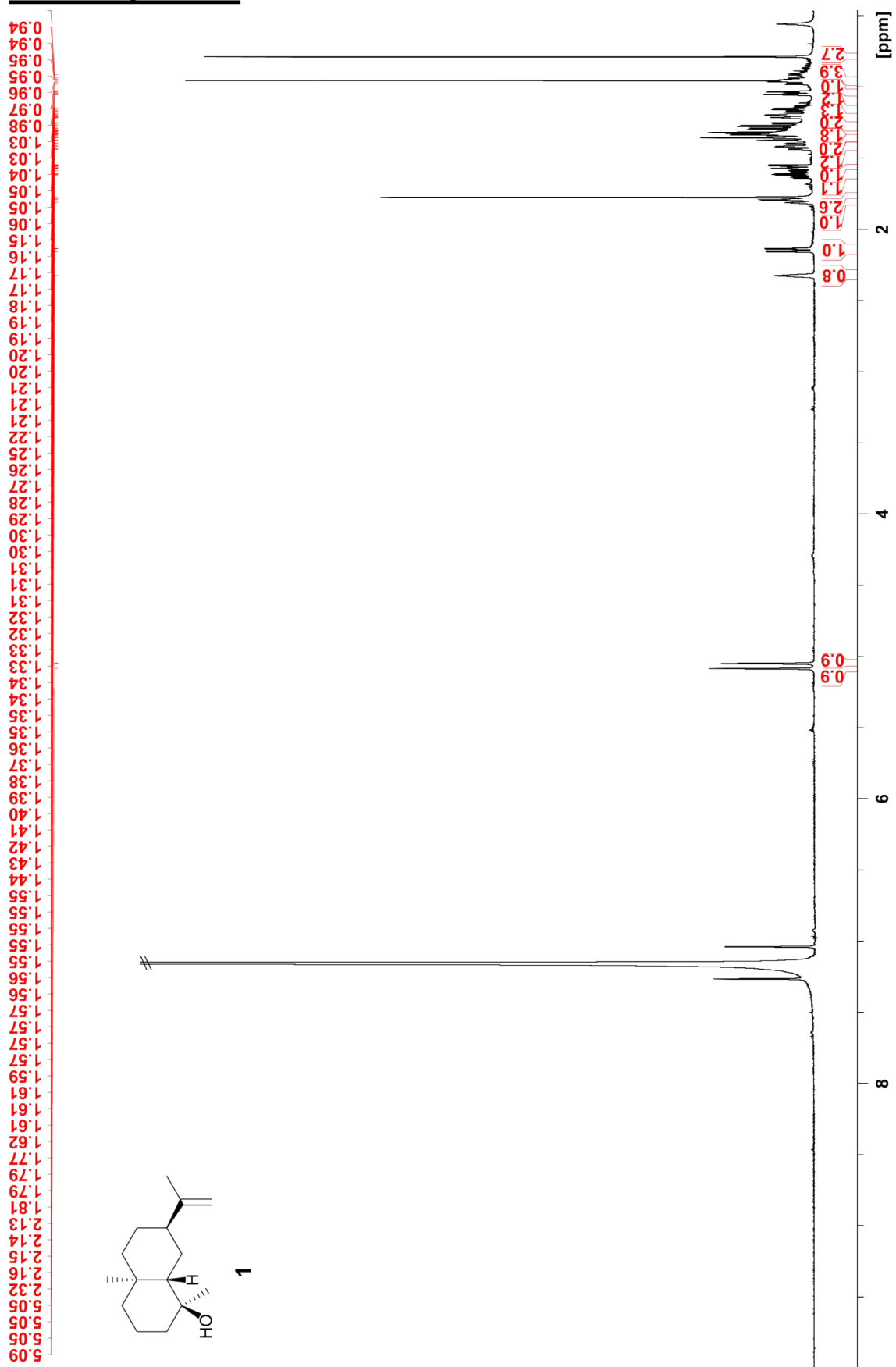


Figure S19: ¹H-NMR spectrum (700 MHz) of **1** recorded in C₆D₆.

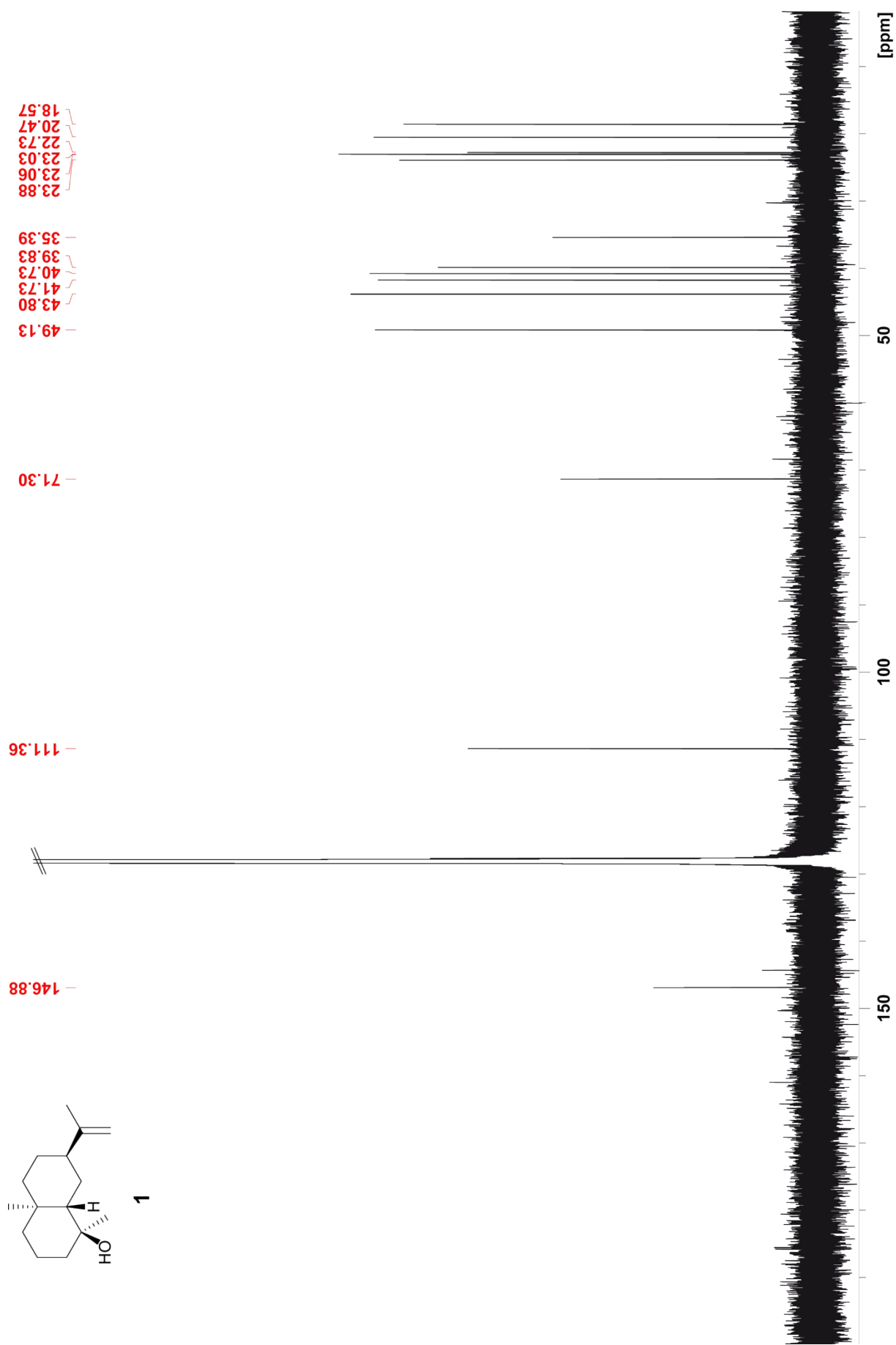


Figure S20: ^{13}C -NMR spectrum (175 MHz) of **1** recorded in C_6D_6 .

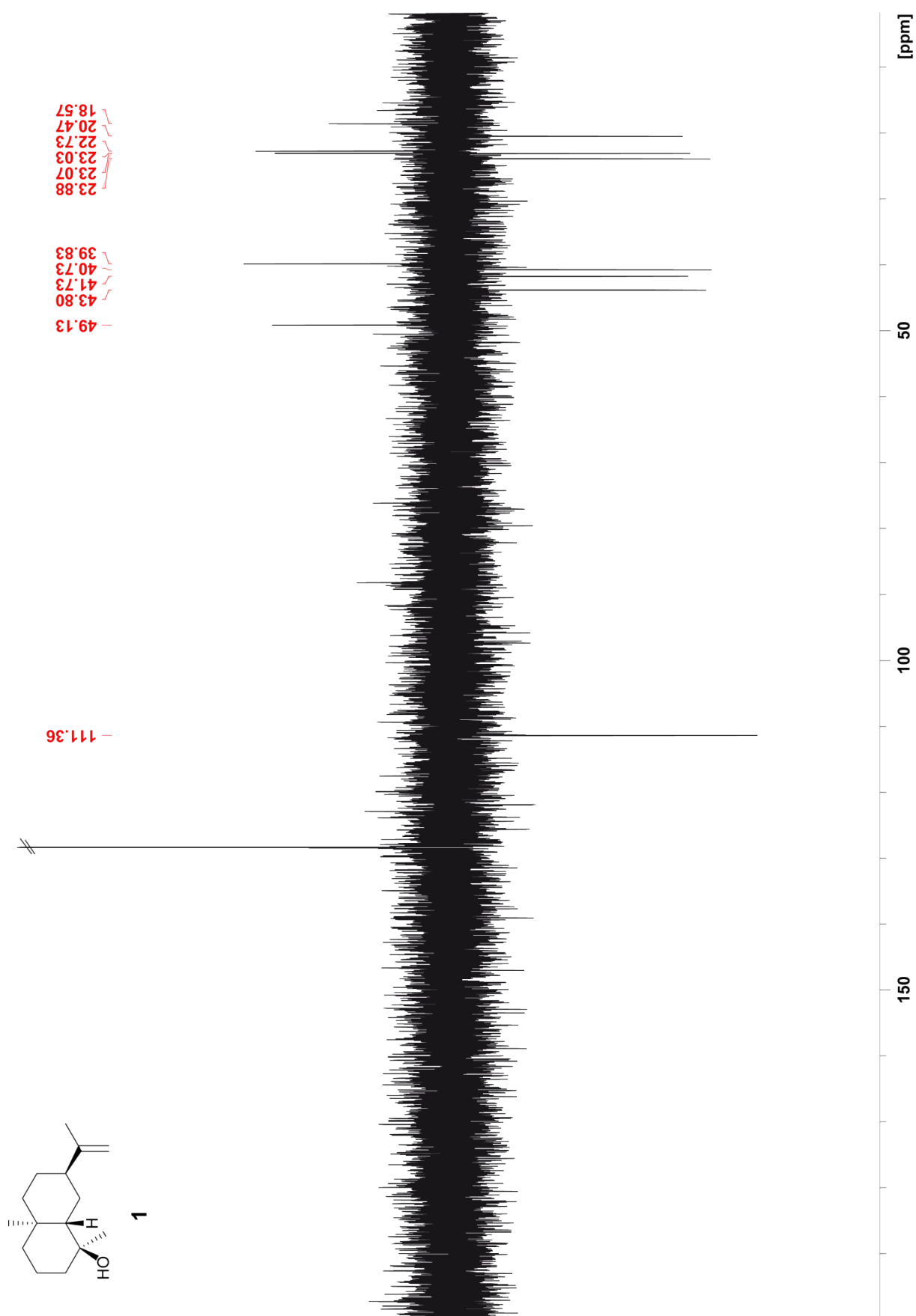


Figure S21: ^{13}C -DEPT spectrum (175 MHz) of **1** recorded in C_6D_6 .

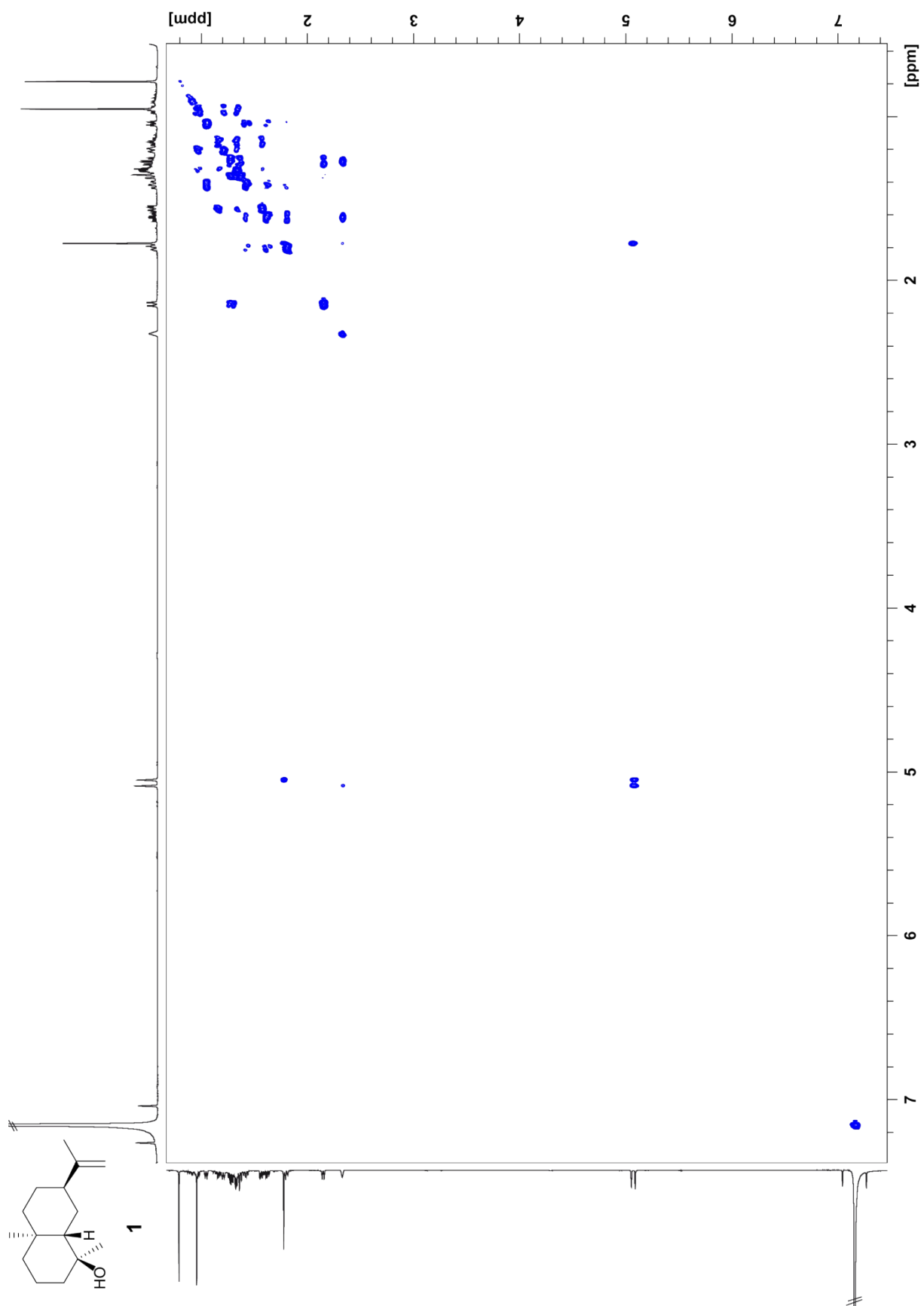


Figure S22: $^1\text{H},^1\text{H}$ -COSY spectrum of **1** recorded in C_6D_6 .

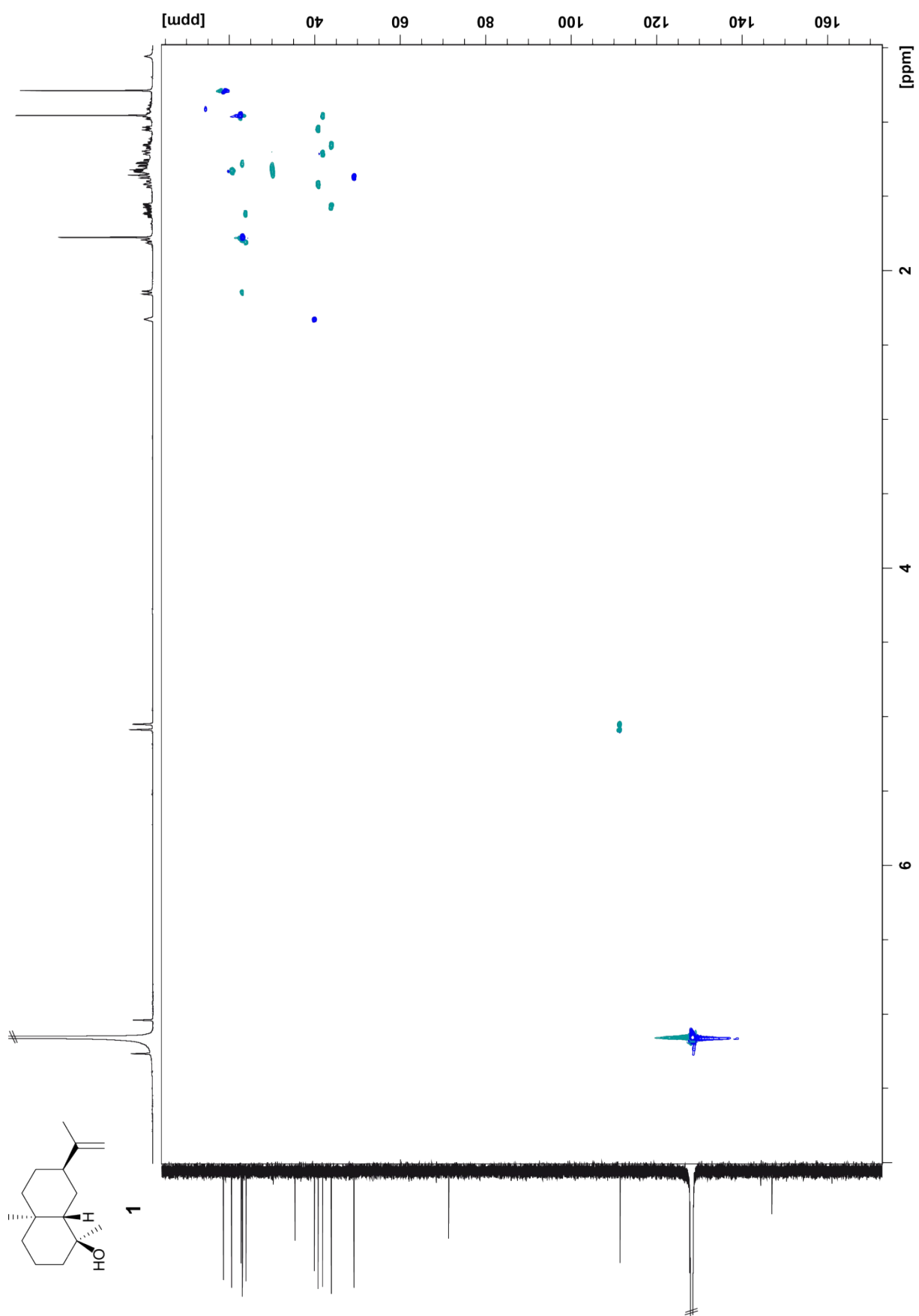


Figure S23: ^1H , ^{13}C -HSQC spectrum of **1** recorded in C_6D_6 .

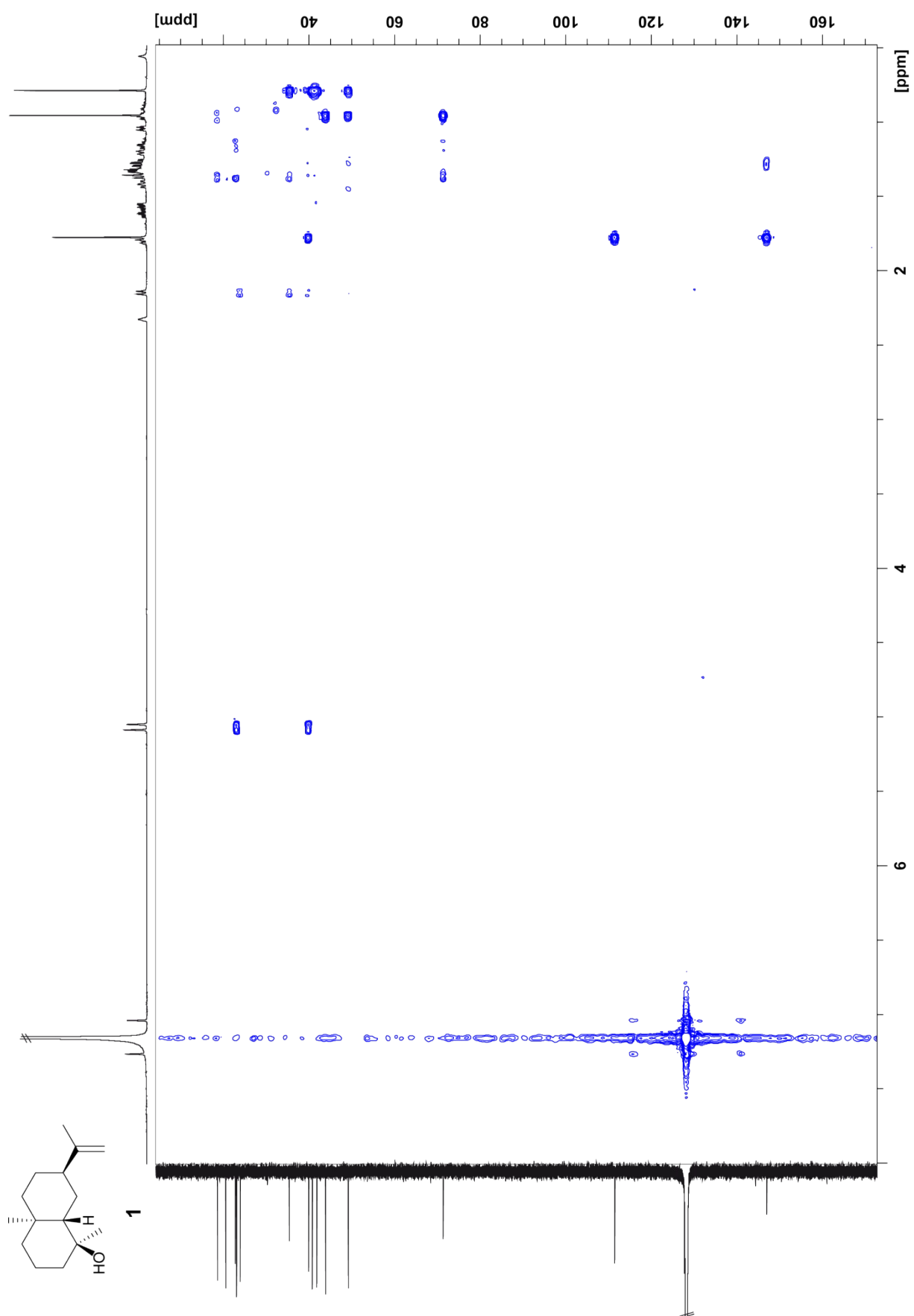


Figure S24: ^1H , ^{13}C -HMBC spectrum of **1** recorded in C_6D_6 .

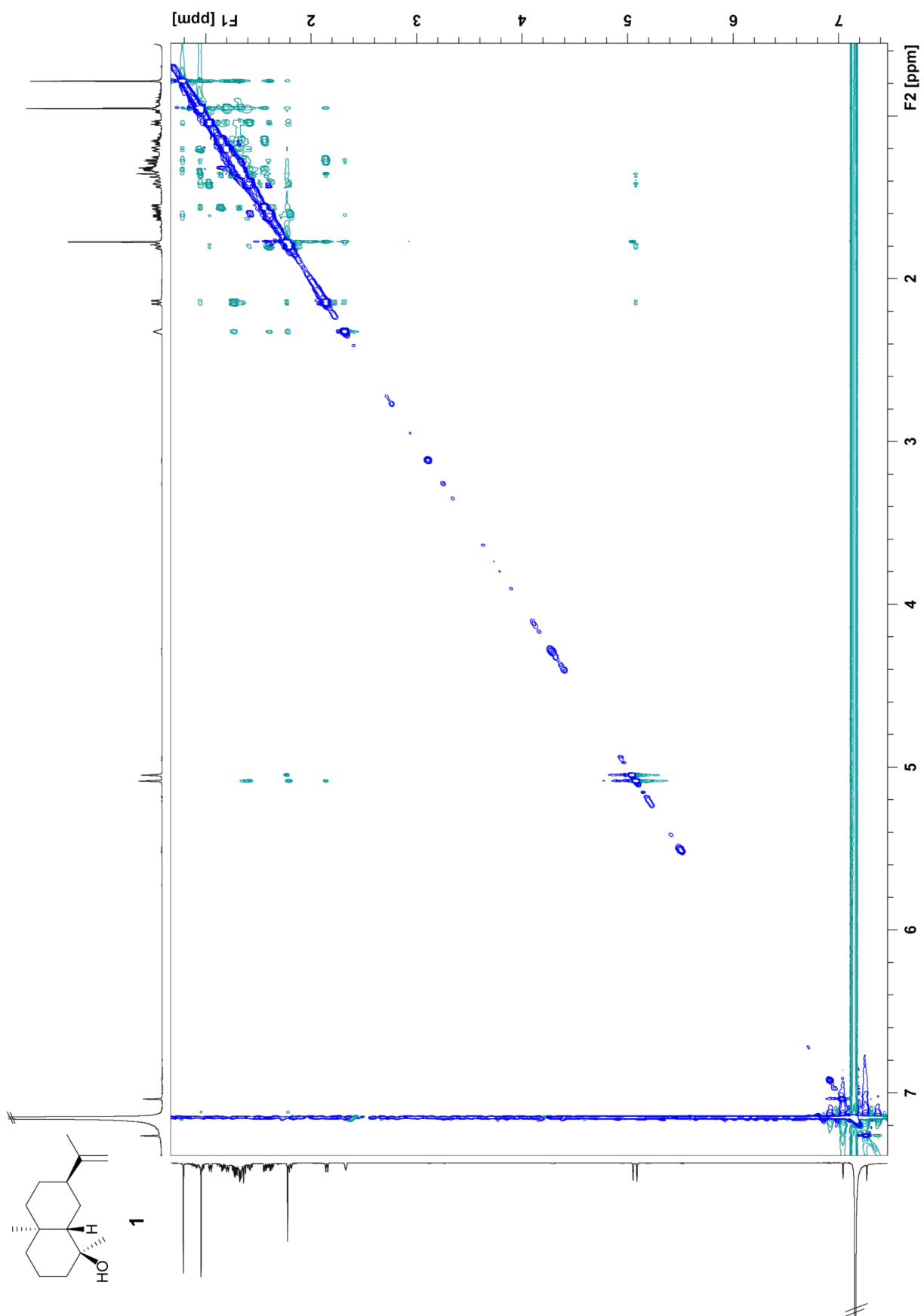


Figure S25: $^1\text{H}, ^1\text{H}$ -NOESY spectrum of **1** recorded in C_6D_6 .

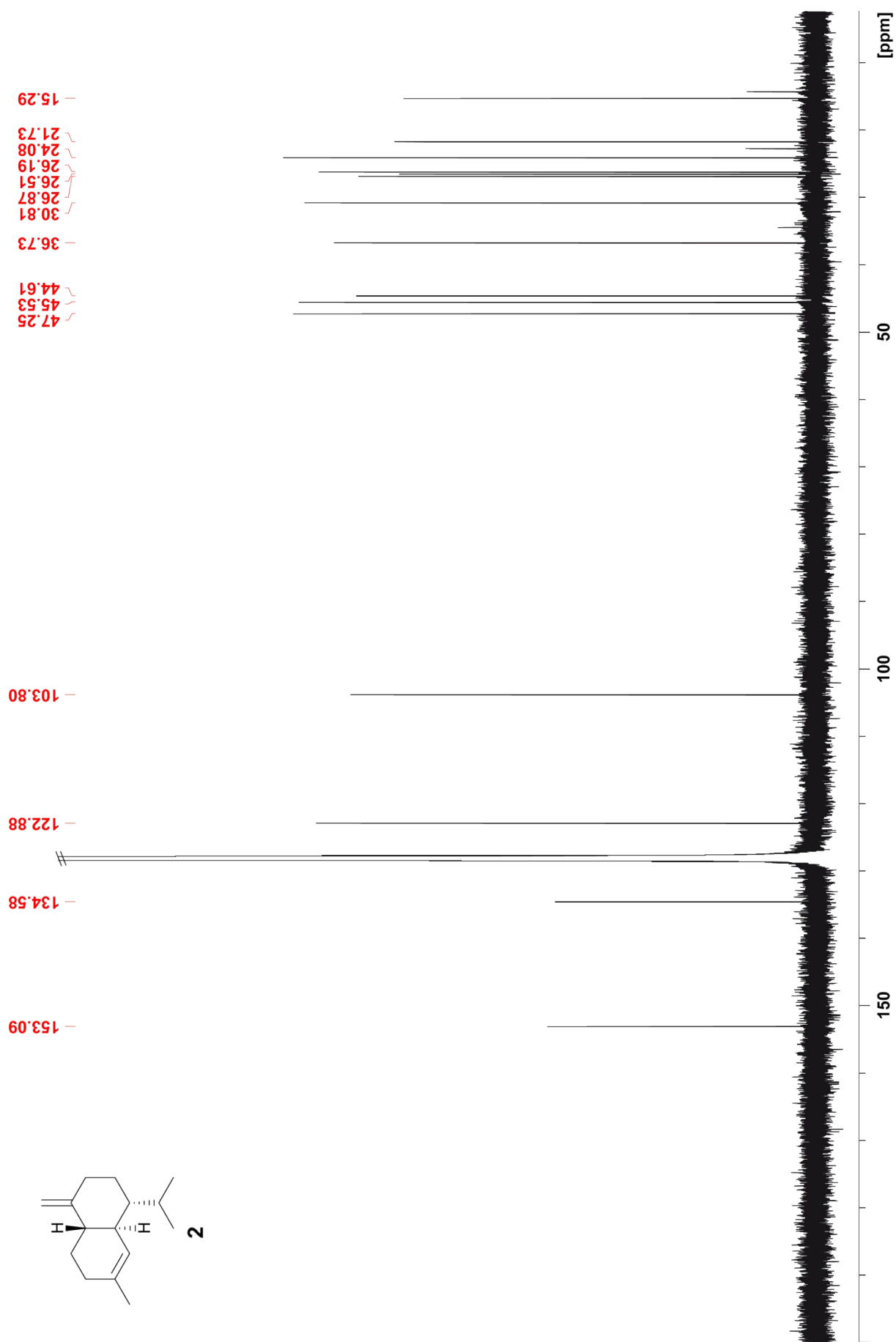


Figure S27: ¹³C-NMR spectrum (175 MHz) of **2** recorded in C₆D₆.

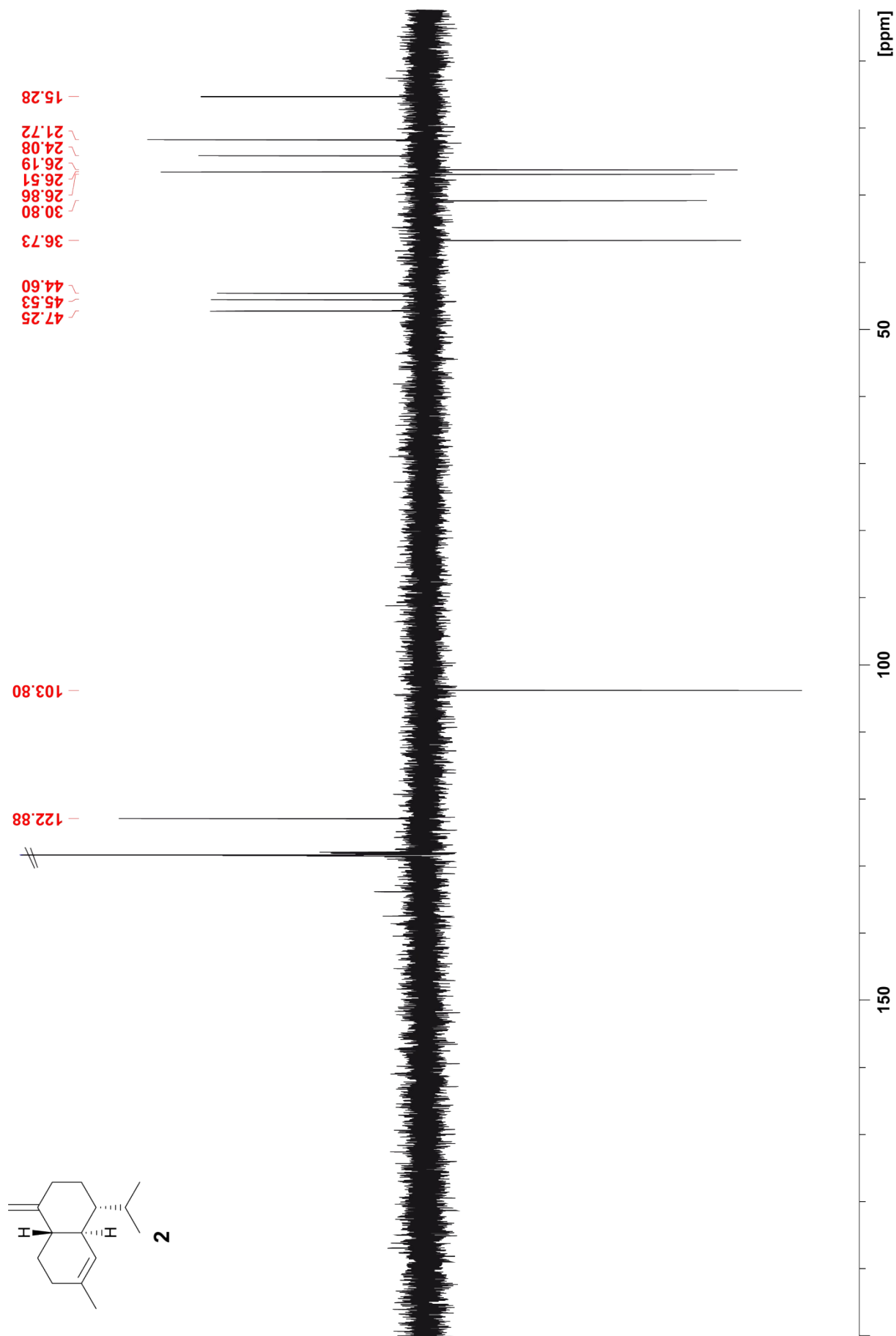


Figure S28: ^{13}C -DEPT spectrum (175 MHz) of **2** recorded in C_6D_6 .

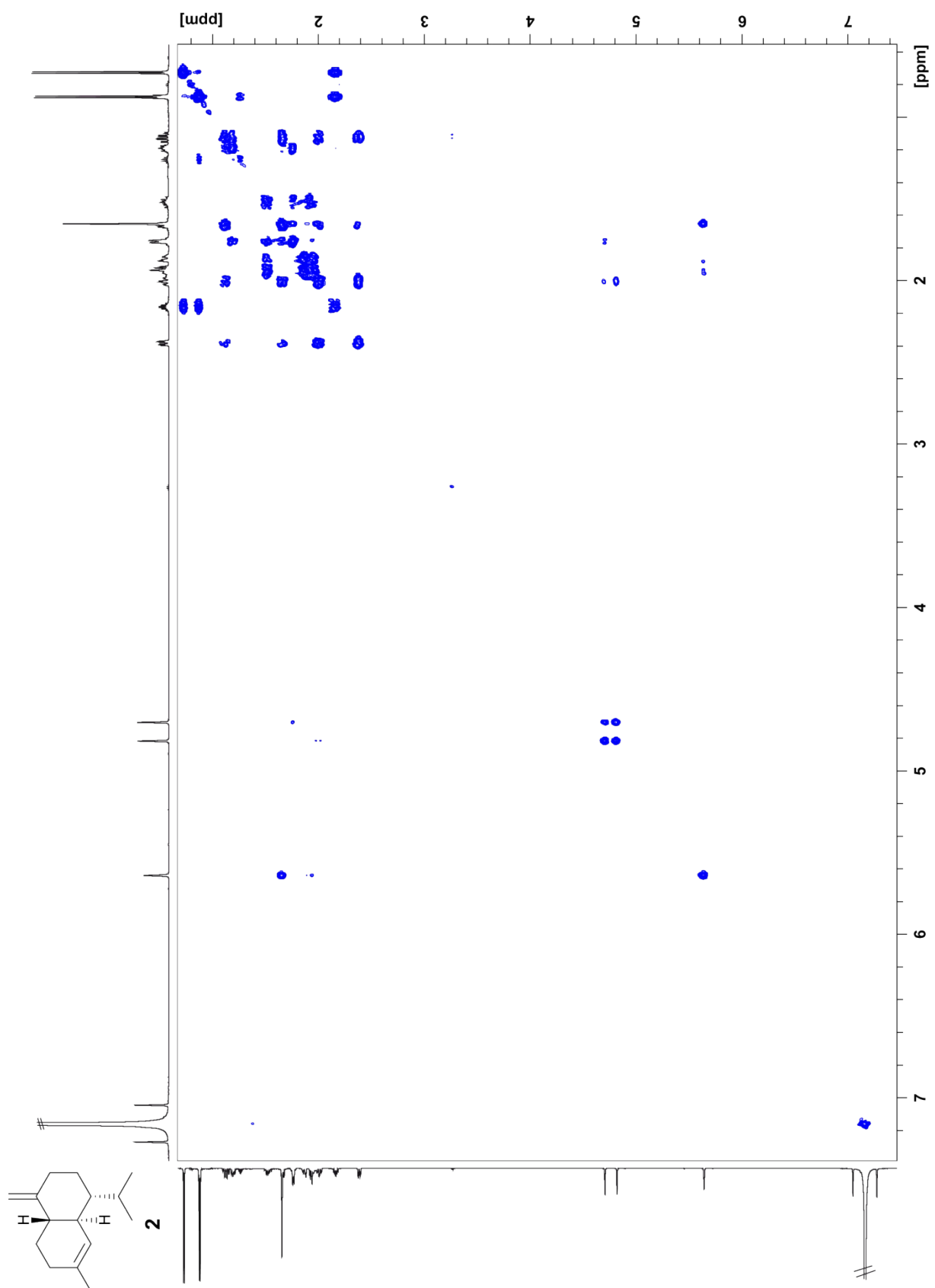


Figure S29: $^1\text{H},^1\text{H}$ -COSY spectrum of **2** recorded in C_6D_6 .

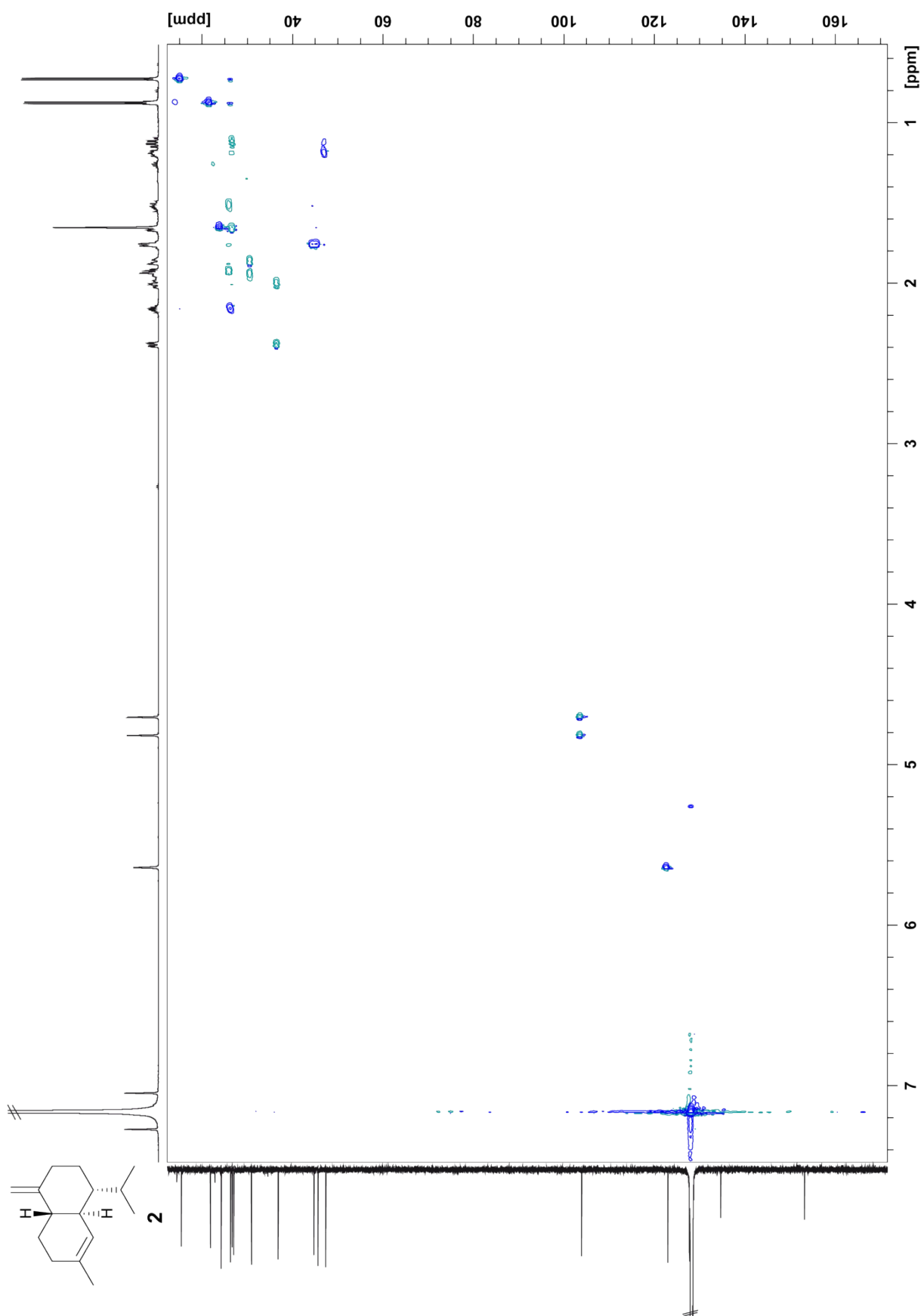


Figure S30: ^1H , ^{13}C -HSQC spectrum of **2** recorded in C_6D_6 .

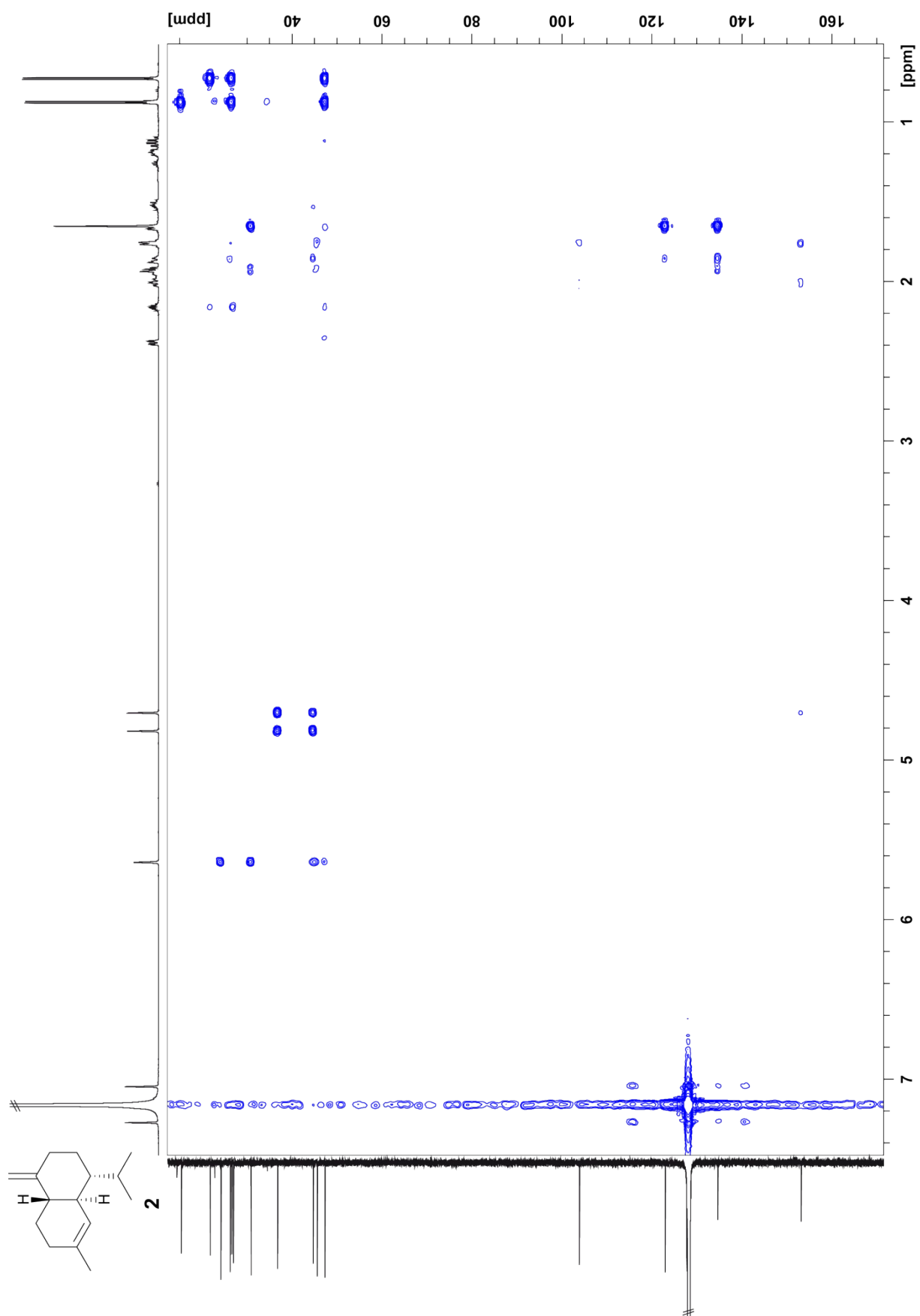


Figure S31: ^1H , ^{13}C -HMBC spectrum of **2** recorded in C_6D_6 .

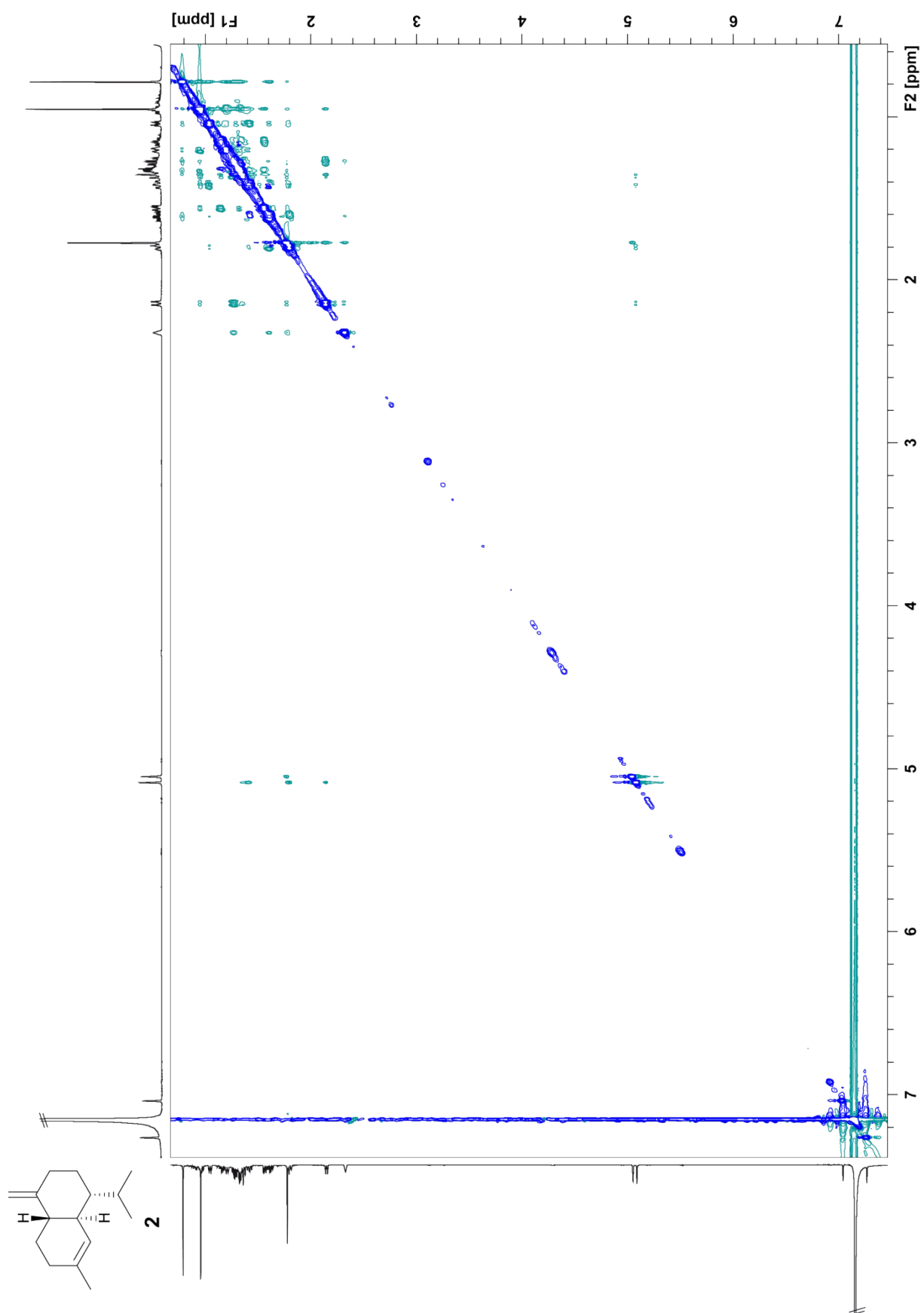


Figure S32: $^1\text{H}, ^1\text{H}$ -NOESY spectrum of **2** recorded in C_6D_6 .

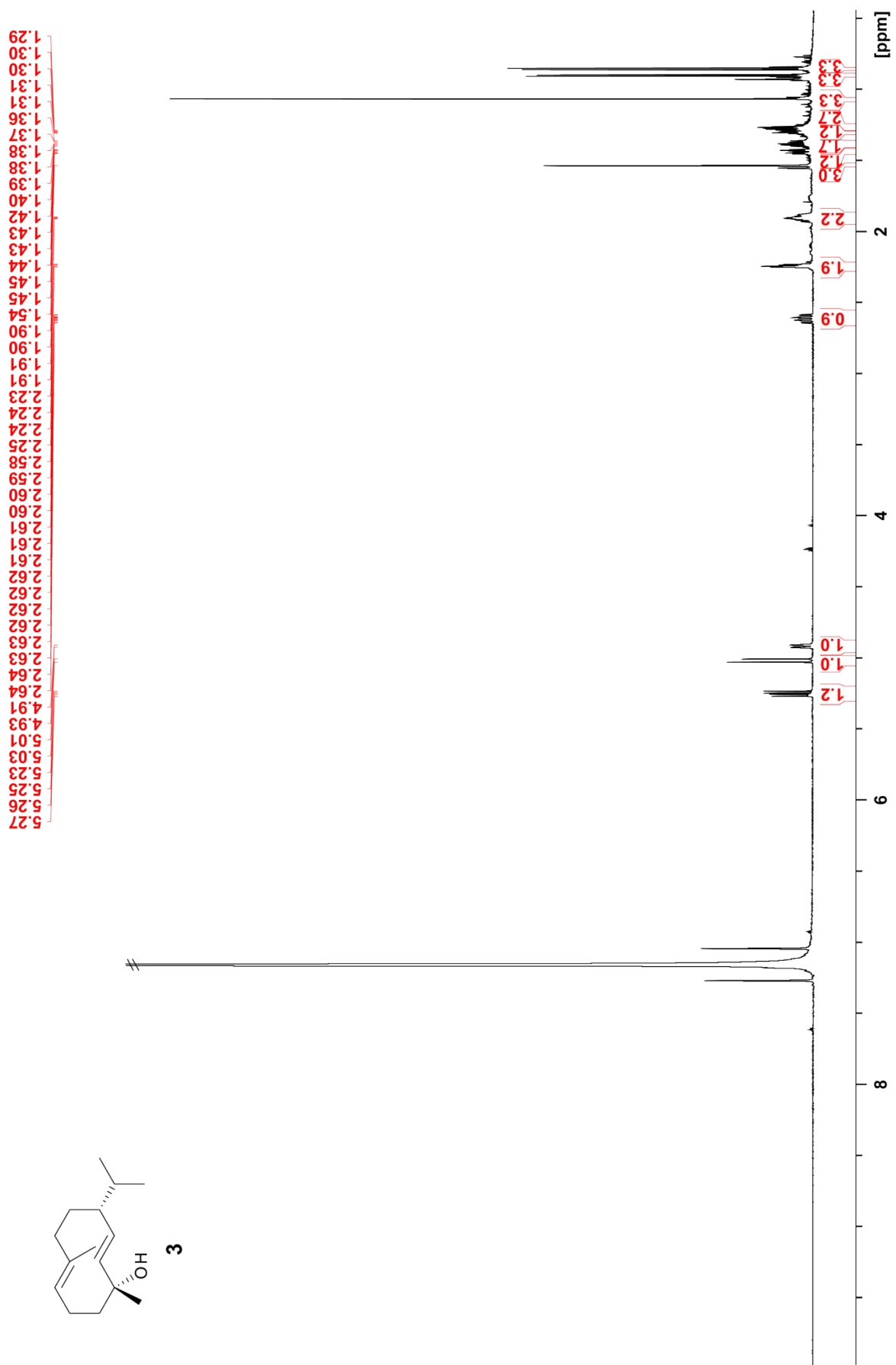


Figure S33: ¹H-NMR spectrum (700 MHz) of **3** recorded in C₆D₆.

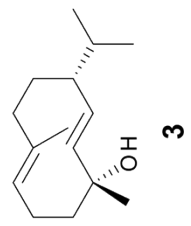
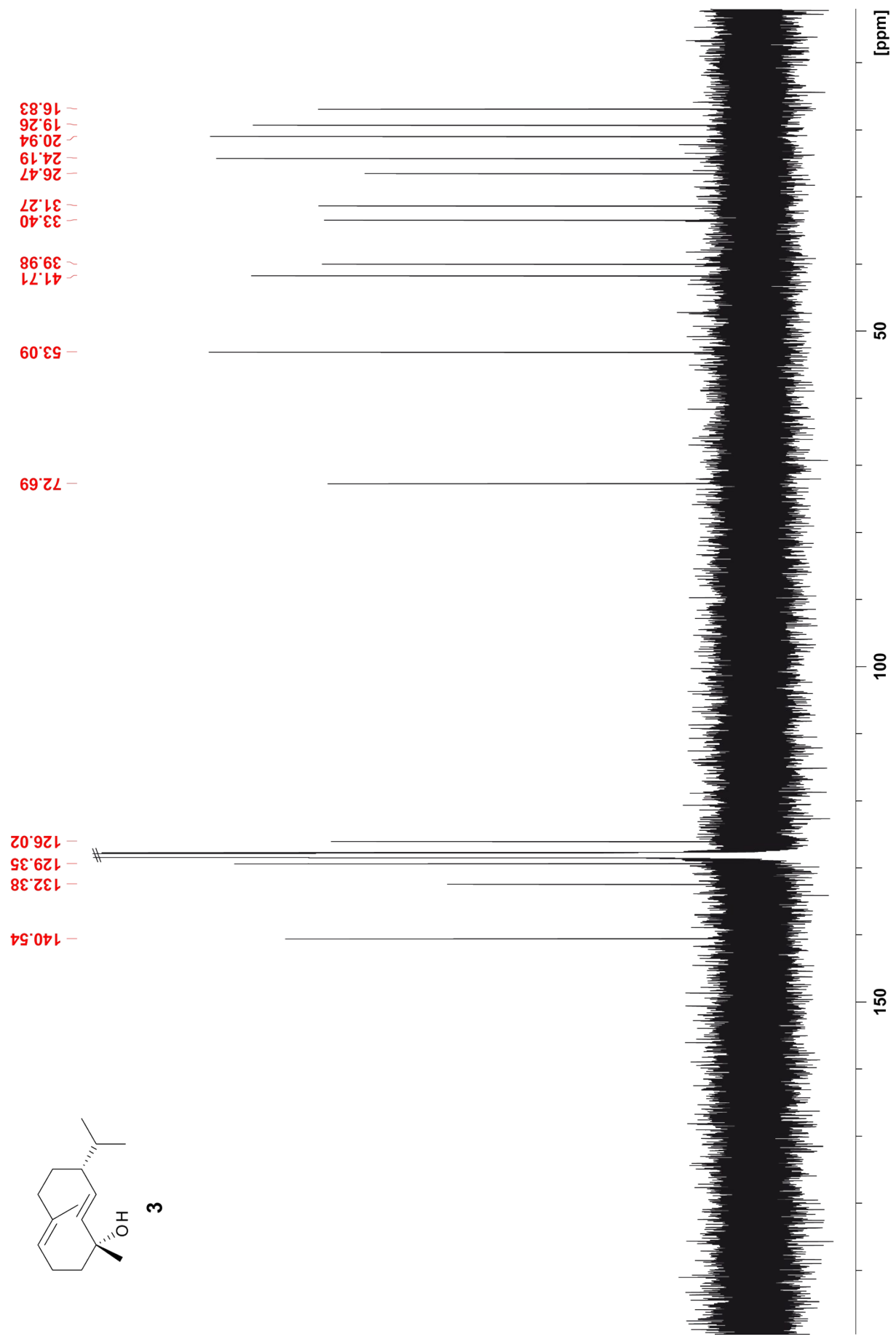


Figure S34: ^{13}C -NMR spectrum (175 MHz) of **3** recorded in C_6D_6 .

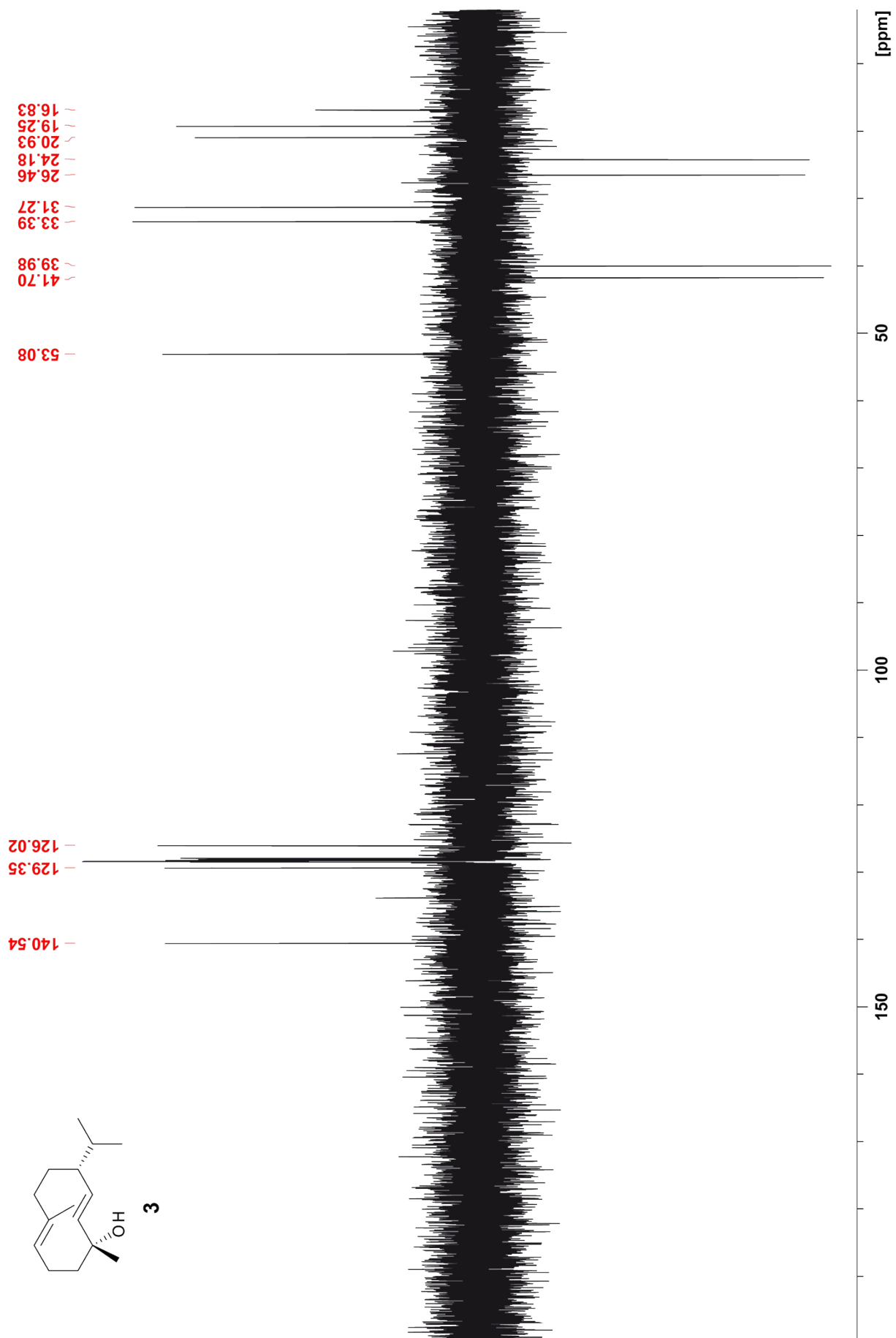


Figure S35: ^{13}C -DEPT spectrum (175 MHz) of **3** recorded in C_6D_6 .

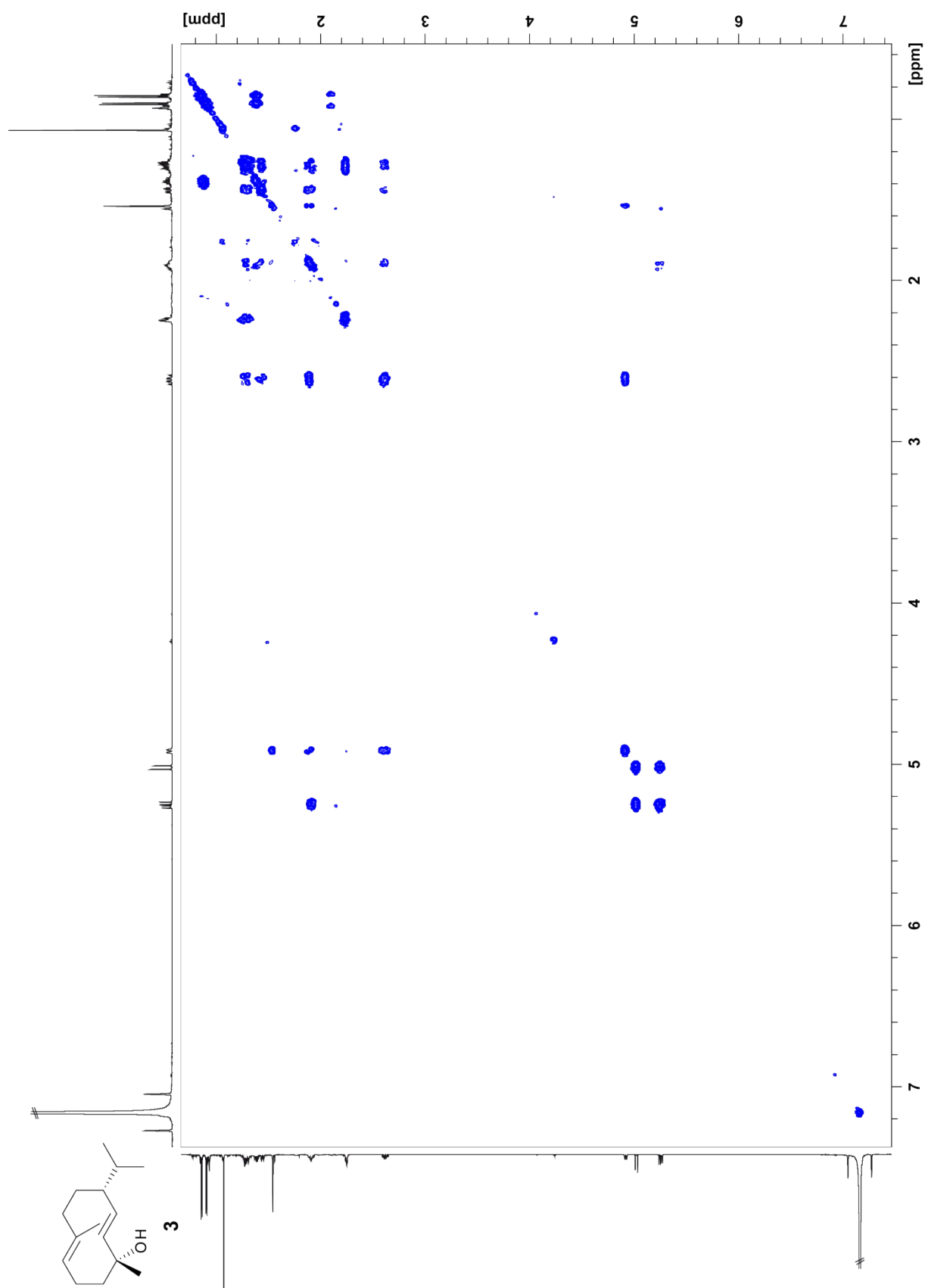


Figure S36: ^1H , ^1H -COSY spectrum of **3** recorded in C_6D_6 .

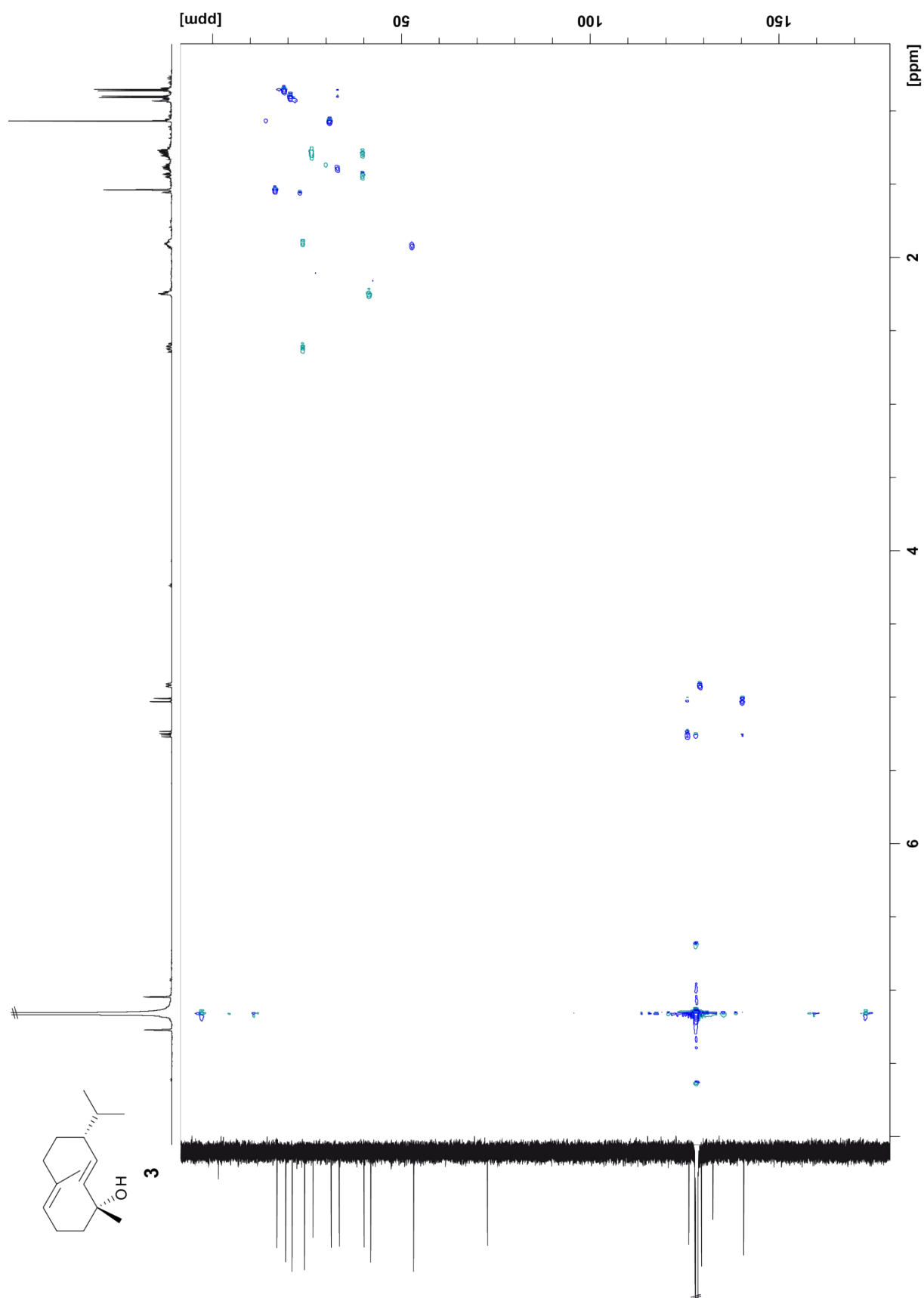


Figure S37: ^1H , ^{13}C -HSCQ spectrum of **3** recorded in C_6D_6 .

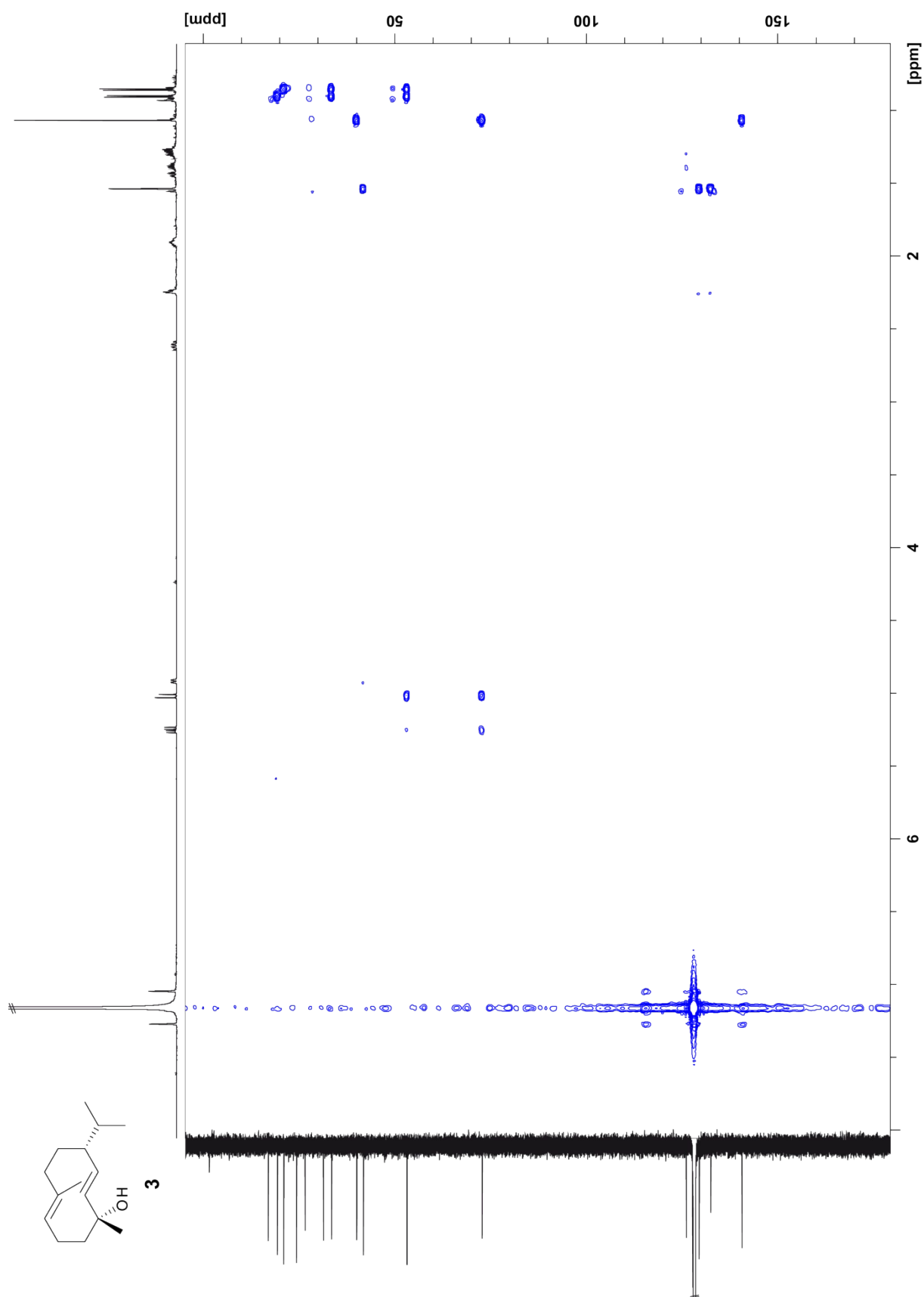


Figure S38: ^1H , ^{13}C -HMBC spectrum of **3** recorded in C_6D_6 .

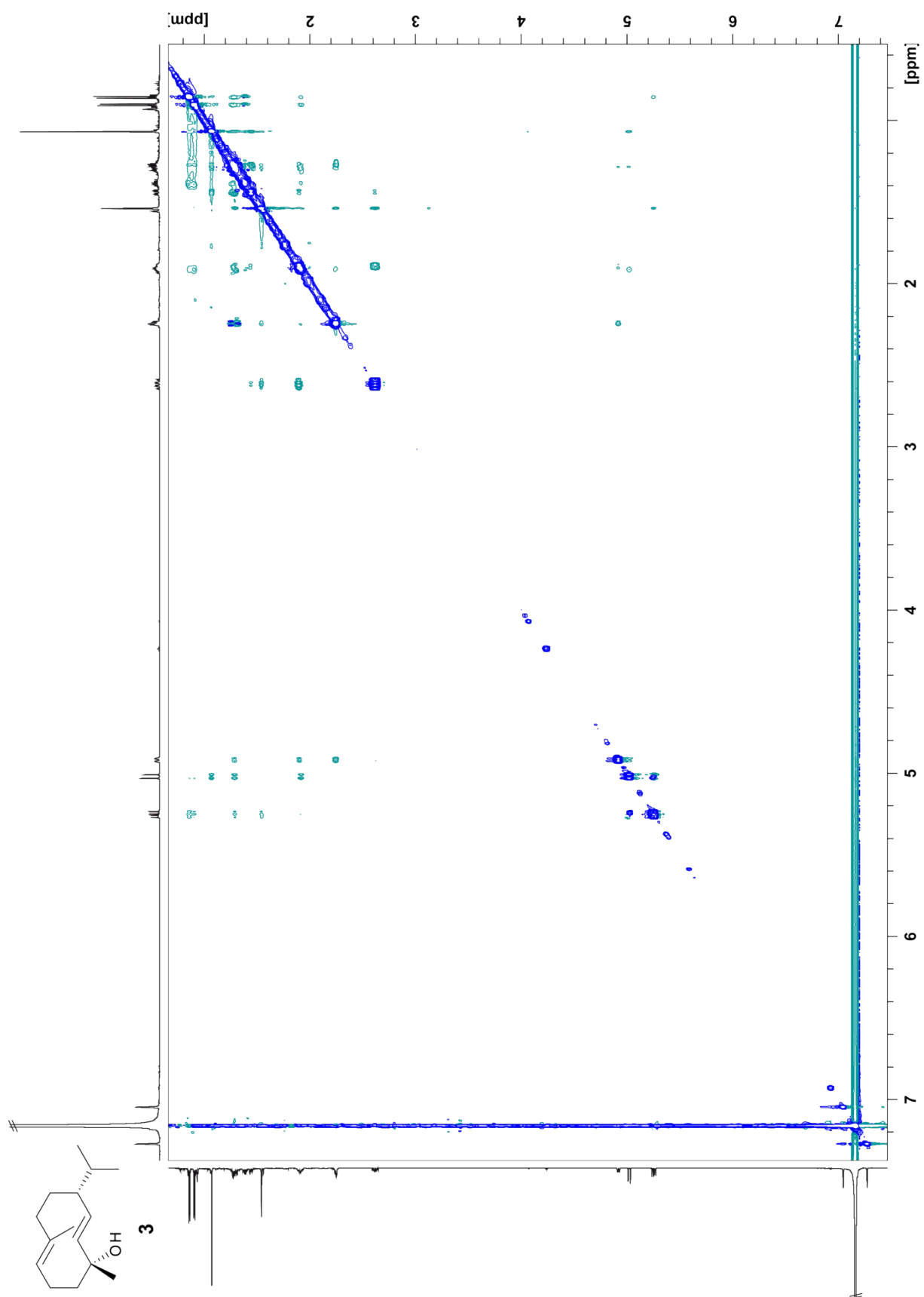


Figure S39: $^1\text{H}, ^1\text{H}$ -NOESY spectrum of **3** recorded in C_6D_6 .

References

- [1] T. Weber, K. Blin, S. Duddela, D. Krug, H. U. Kim, R. Bruccoleri, S. Y. Lee, M. A. Fischbach, R. Müller, W. Wohlleben, R. Breitling, E. Takano and M. H. Medema, *Nucl. Acids Res.*, 2015, **43**, W1, W237-W243.
- [2] J. S. Dickschat, K. A. K. Pahirulzaman, P. Rabe and T. A. Klapschinski, *ChemBioChem*, 2014, **15**, 810-814.
- [3] R. D. Giets and R. H. Schiestl, *Nat. Protoc.*, 2007, **2**, 31–34.
- [4] (a) C. A. Citron, P. Rabe, L. Barra, C. Nakano, T. Hoshino and J. S. Dickschat, *Eur. J. Org. Chem.*, 2014, 7684-7691; (b) J. Rinkel, P. Rabe, P. Garbeva and J. S. Dickschat, *Angew. Chem. Int. Ed.*, 2016, **55**, 13593-13596.
- [5] P. Rabe, J. Rinkel, T. A. Klapschinski, L. Barra and J. S. Dickschat, *Org. Biomol. Chem.*, 2016, **14**, 158-164.
- [6] P. Rabe, T. Schmitz and J. S. Dickschat, *Beilstein J. Org. Chem.*, 2016, **12**, 1893-1850.
- [7] D. Arigoni, *Pure Appl. Chem.*, 1975, **41**, 219-245.
- [8] P. Baer, P. Rabe, K. Fischer, C. A. Citron, T. A. Klapschinski, M. Groll and J. S. Dickschat, *Angew. Chem. Int. Ed.*, 2014, **53**, 7652-7656.
- [9] Y. Hu, W. K. W. Chou, R. Hopson and D. E. Cane, *Chem. Biol.*, 2011, **18**, 32-37.